

DEC 3 1963

UNCLASSIFIED
DRAGON PROJECT USE ONLY

D. P. Report 227

7243

O.E.C.D. HIGH TEMPERATURE REACTOR PROJECT

DRAGON



Dragon Project Report

PRELIMINARY REPORT

THE IRRADIATION BEHAVIOUR OF COATED PARTICLE FUEL

LEGAL NOTICE

This report has been released from the United States Atomic Energy Commission by the United Kingdom Atomic Energy Authority under an agreement for cooperation with the understanding that the position of the United Kingdom regarding legal responsibility is identical to that of the United States, which is stated as follows: Neither the United States, nor the Commission, nor any person acting on behalf of the Commission:

A. Makes any warranty or representation, expressed or implied, with respect to the accuracy, completeness, or usefulness of the information contained in this report, or that the use of any information, apparatus, method, or process enclosed in this report may not infringe privately owned rights; or

B. Assumes any liabilities with respect to the use of, or for damages resulting from the use of any information, apparatus, method, or process disclosed in this report.

As used in the above, "person acting on behalf of the Commission" includes any employee or contractor of the Commission, or employee of such contractor, to the extent that such employee or contractor of the Commission, or employee of such contractor prepares, disseminates, or provides access to, any information pursuant to his employment or contract with the Commission, or his employment with such contractor.

by

J. B. SAYERS
 K. S. B. ROSE
 J. H. COOBS
 G. P. HAUSER
 C. VIVANTE

Facsimile Price \$ ~~27.50~~Microcard Price \$ ~~17.00~~
for Access Permittees

Available from the
 Division of Technical Information Extension
 P. O. Box 1061
 Oak Ridge, Tennessee

This paper is to be presented at the Harwell
 Symposium on Carbide in Nuclear Energy,
 on 5th, 6th and 7th November, 1963

NOTICE

This report was received under the provisions
 of the USAEC Dragon Project
 arrangement and is subject to the terms thereof.

The above distribution limitation was placed
 on this report when transmitted to the USAEC
 by the British Government.

A.E.E. Winfrith, Dorchester, Dorset, England

October, 1963

UNCLASSIFIED

DISCLAIMER

This report was prepared as an account of work sponsored by an agency of the United States Government. Neither the United States Government nor any agency thereof, nor any of their employees, makes any warranty, express or implied, or assumes any legal liability or responsibility for the accuracy, completeness, or usefulness of any information, apparatus, product, or process disclosed, or represents that its use would not infringe privately owned rights. Reference herein to any specific commercial product, process, or service by trade name, trademark, manufacturer, or otherwise does not necessarily constitute or imply its endorsement, recommendation, or favoring by the United States Government or any agency thereof. The views and opinions of authors expressed herein do not necessarily state or reflect those of the United States Government or any agency thereof.

DISCLAIMER

Portions of this document may be illegible in electronic image products. Images are produced from the best available original document.

THE IRRADIATION BEHAVIOUR OF COATED PARTICLE FUEL

by

* J. B. SAYERS
* K. S. E. ROSE
** J. H. COOBS
*** G. P. HAUSER
*** C. VIVANTE

ABSTRACT

Irradiation experiments have been carried out both within the Dragon Project and at A.E.R.E. on a variety of carbide fuels coated with either pyrocarbon or composite pyrocarbon-SiC coatings. Both static capsule and gas cooled loop experiments have been performed covering a range of burn-ups up to 14% of initial metal atoms.

In the higher burn-up range, covering up to 14% of initial metal atoms (2×10^{21} fission/cm³), all the particles had fully enriched sintered "UC₂" kernels with porosities in the range 30-50%. They were coated with two or three distinct pyrocarbon coatings, and tested both in compact form and as unsupported particles. The results show that this type of particle can withstand a burn-up of 8% at temperatures below 1300°C with very low failure rate. Above 8% burn-up the data are solely from particles in compacts and although failure can normally be attributed to an advanced form of "spearhead" attack, there is also some evidence to suggest that this had been aggravated by external corrosive effects.

In the lower burn-up range, up to 2.6% of initial metal atoms (3×10^{20} - 10^{21} fission/cm³ depending on kernel type and density), both sintered and melted (Th,U)C₂ and melted (Zr,U)C particles coated with a triplex pyrocarbon coat have been irradiated at temperatures up to 1400°C only in compact form. Sintered (Zr,U)C particles coated with various types of pyrocarbon coatings have been irradiated similarly at temperatures up to 1700°C. The melted (Th,U)C₂ kernels cracked under irradiation causing stress cracking in all the coating layers, whereas in the sintered type no failed coatings were found nor were any diffusional effects observed in the SiC layer. The melted (Zr,U)C kernels did not show this cracking, but metallographic examination showed them to be polycrystalline and less dense than the thorium containing kernels. No diffusion of the sintered (Zr,U)C into the pyrocarbon coating was observed in spite of the high irradiation temperatures.

Only tentative comparisons between pyrocarbon and composite pyrocarbon-SiC as coatings, or UC₂ as opposed to "alloyed" kernels are possible with the present data, as the burn-up and temperature ranges covered hardly overlap.

Two phenomena which appear to have a marked influence on particle behaviour are discussed in some detail:-

- (1) The occurrence of a low temperature sintering phenomenon attributable to irradiation.

*Metallurgy Division, A.E.R.E., Harwell
**Oak Ridge National Laboratory, attached to Dragon Project
***Dragon Project

(2) The so-called "spearhead" attack in pyrocarbon which is tentatively ascribed to fission fragment recoil damage causing ordering and possibly graphitisation of the pyrocarbon, resulting in a shrinkage. The initiation of the cracks in the pyrocarbon coating may be due to chemical attack by fission products.

CONTENTS

	<u>PAGE NO.</u>
1. INTRODUCTION	7
2. TYPES OF FUEL PARTICLES TESTED IN THIS PROGRAMME	8
2.1 Pre-Irradiation Evaluation of Particles	8
2.2 Types of Irradiation Tests	9
3. FISSION PRODUCT RELEASE RESULTS	9
4. RESULTS OF MICROSCOPIC EXAMINATION	11
4.1 Fuel Kernels	11
4.1.1 UC_2 Kernels	11
4.1.1.1 Phases in Fuel Kernel	12
4.1.1.2 Sintering and Swelling	13
4.1.2 $(Th,U)C_2$ Kernels	15
4.1.3 $(Zr,U)C$ Kernels	15
4.2 Coatings and Interactions between Fuel and Coating	16
4.2.1 Pyrocarbon Coatings	16
4.2.1.1 Diffusional Effects	16
4.2.1.2 Spearhead Attack and Shrinkage of Pyrocarbon	20
4.2.1.3 Other Cracking Phenomena	22
4.2.2 Triplex Coatings (Pyrocarbon/Silicon Carbide/Pyrocarbon)	23
5. DISCUSSION ON THE FACTORS AFFECTING PARTICLE INTEGRITY	24
5.1 Volume Changes in the Kernel	24
5.2 Fission Product Release	25
5.3 Fuel Phase Composition	27
5.4 Temperature and Burn-up	28
5.4.1 Temperature Effects	28
5.4.2 Burn-up and Rate of Burn-up	29
5.5 Coating Structure	30

5.6 Fission Fragment and Fast Neutron Damage to Pyrocarbon and Silicon Carbide	31
6. SUMMARY AND CONCLUSIONS	34
7. ACKNOWLEDGMENTS	35
8. REFERENCES	36

LIST OF ILLUSTRATIONS

FIGURE

1. DY; Unirradiated Particle (X250).
2. PL IIIA/2; Typical Particle (X250).
3. DY7; Typical Particle (X250).
4. PL IIIA/5; Typical Particle (X250).
5. PL IIIA/1; Details of Structure of Kernel and Spearhead Attack (X570).
6. PL IIIA/2; Structure of Kernel (X1000).
7. PL IIIA/7; Large Spearheads Penetrating the Coating (X250).
8. DY5; Diffusion of Fuel into Coating; Kernel has a Low Density and has an Inclusion of Graphite at its Centre (X250).
9. HPD2/3; Diffusion of Fuel and Coating (X250).
10. PL IIIA/5; Details of Fine Precipitate in Carbide Phase (X250).
11. P1; Broken Particle (X190).
12. HPD4/3A; Structure of Partially Recrystallised Kernel (X380).
13. HPD4/2A; Structure of Un-Recrystallised Kernel (X350).
14. HPD4/4B; Typical Particle (X150).
15. DY; Unirradiated, Showing Diffusion of Fuel Through Coating at 2200°C (X240).
16. PL IIIA/7; Diffusion Zone Extending 5μ (X250).
- 17a. DY1; Diffusion of Fuel into Coating (X250).
- 17b. DY1; As Fig. 17a under Polarised Light (X250).
18. PL IIIA/9; Severe Lamination of Coating Caused by External Corrosion (X250).

FIGURE

19. Characteristic Shape of Spearhead Attack (X275).
20. DY7; Spearhead Attack and Swelling of Kernel into Voids (X250).
21. P1; Microradiograph Showing Spearhead Attack (X160).
- 22a. DY1; Particle Under White Light (X250).
- 22b. DY1; As Fig. 22a Under Polarised Light (X250).
23. HPD5; Coating Type C201, Unirradiated (X160).
24. HPD5; Coating Type C200, Unirradiated (X160).
25. HPD5; Coating Type C203, Unirradiated (X160).
26. HPD5; Coating Type C202, Unirradiated (X160).
27. HPD5/5A; Penetration of Spearhead Attack into Outer Columnar Coatings (X154).
28. HPD5/3A; Spearhead Attack Limited to Inner Coating (X154).
29. HPD5/5B; Coatings Fractured by Wide Radial Cracks (X154).
30. HPD5/6A; Hairline Cracks in Coating (X154)
31. HPD4/3B; Intact Kernel, Cracks in SiC Often Correspond with Tips of Spearheads in Inner PyC Layer (X150).
32. Plot of Ratio of Release Rate to Birth Rate of Fission Gases versus Half-Life for Studsvik I.

LIST OF TABLES

TABLE

1. Summary of Fuel Charge Details.
2. Summary of Failures on Pyrocarbon Coated Particles.
3. Summary of Failures on Triplex Pyrocarbon/SiC/Pyrocarbon Coated Particles.
4. Details of Pyrocarbon Coated UC_2 Particles for P1, DY and HPD2 Charges.
5. Details of Particles in HPD4 Charge.
6. Details of Pyrocarbon Coated $(Zr,U)C$ Particles Irradiated in HPD5.
7. Details of Pyrocarbon Coated UC_2 Particles Irradiated in Pluto Loop Charge IIIA.
8. Details of Particles in Studsvik I Charge.



THE IRRADIATION BEHAVIOUR OF COATED PARTICLE FUEL

by

* J. B. SAYERS
* K. S. B. ROSE
** J. H. COOBS
*** G. P. HAUSER
*** C. VIVANTE

INTRODUCTION

The advantages of retention of fission products in the fuel phase were realised in the early days of the Dragon Project, and ideas for preventing their escape by various methods of coating fuel particles were worked on as part of the early Research and Development work. When it was demonstrated by the Battelle workers [1] in 1960 that alumina coated particles of UO_2 could withstand irradiation and retain a large proportion of the fission product gases, a major programme on the coated particle fuel concept was started using carbide fuel with pyrocarbon coatings deposited in a fluidised bed. Since that date a large amount of work has been carried out on this type of fuel as evidenced by the bulk of data presented at the BMI Symposium in November, 1962 [2].

Naturally the fabrication development has progressed far more rapidly than the ability to carry out irradiation tests to the required burn-up levels. The initial objective was to produce a particle which exhibited a high retention of the fission gases on post-irradiation annealing of lightly irradiated material, since the question of which were the most important parameters involved in the retention of particle integrity to high burn-ups was largely a matter of intuitive guesses.

Due to the need to obtain sufficient data to define the fuel particle fabrication route for the first charge of the Dragon reactor by September, 1963, the tests described in this paper are largely of a technological nature, as in fact are most of the published data. Burn-up and irradiation temperature have, however, been varied (though not in all cases independently) over a wide range.

The development of a completely new fuel concept, i.e., pyrocarbon or pyrocarbon/silicon carbide coated $(Th,U)C_2$ or $(Zr,U)C$, without the basic data on either fuel or coating material has made interpretation of the high burn-up results difficult. The highest burn-up reported on bulk carbide fuel is 2.5% and was obtained on UC, [3, 4] at lower temperatures than those of interest to high temperature gas cooled reactors, cf., burn-ups up to 14% reported in this paper.

The data on fast neutron damage to pyrocarbon are very sparse [5] and only one experiment on fission fragment damage is reported [6]. Both sets of experiments have been carried out at temperatures and to doses so different from the conditions existing in these fuels as to be of little use in interpreting the observed phenomena. Hence, although certain technological questions can now be answered, these experiments have posed at least as many new questions on the mechanisms which lead to failure in a coated particle, and many of the tentative explanations put forward require additional definitive experiments to substantiate them.

* Metallurgy Division, A.E.R.E., Harwell
** Oak Ridge National Laboratory, attached to Dragon Project
*** Dragon Project

2. TYPES OF FUEL PARTICLES TESTED IN THIS PROGRAMME

The Dragon Project has a dual objective of both developing a fuel for a large power reactor and, more immediately, to produce a fuel charge for the reactor experiment at Winfrith. In a power reactor the fissile to fertile ratio will be in the range 1:10 to 1:20, but criticality would not be achieved using these ratios because of the small size of the Dragon reactor core; therefore, in order to test elements of the correct composition only a portion of the Dragon elements will contain thorium, and a second type of fuel having a low cross section diluent, namely zirconium, has been developed for the remainder. In addition to the high burn-up experiments with undiluted UC_2 , tests have been performed with both $(Th,U)C_2$ and $(Zr,U)C$ fuel kernels.

Most of these fuel kernels have been coated with varying forms of pyrocarbon. Tests have also been carried out with particles having a triplex coating, i.e., a SiC coating sandwiched between two pyrocarbon layers, as it has been shown in light irradiation tests that the barium and strontium release through silicon carbide is markedly lower than pyrocarbon [7]. Contrary to most of the U.S. work the majority of the kernels have been of the sintered type. The ideal fuel kernel is probably a fused one, so that diffusional release of fission products is minimised, but with sufficient voidage around it to permit it to swell without stressing the coating. As such a particle is difficult to fabricate the next choice seemed to be a porous particle, because although the fission gas release from the fuel is likely to be higher, there is sufficient built-in voidage to accommodate solid fission product swelling. This principle had already been demonstrated in UO_2 by the Bettis workers [8]. Calculations by one of the authors [9], assuming a pessimistic estimate of the swelling rate and complete release of all the volatile fission products from the fuel kernel, suggested that 25-30% voidage would be sufficient to accommodate the expansion expected after 10% burn-up of all atoms at 1500°C. Some fused particles have also been tested to compare their metallurgical behaviour with sintered particles.

Many of the details of the preparation of fuel particles for the various experiments are given in Tables 4-8.

2.1 Pre-Irradiation Evaluation of Particles

The procedures adopted are mainly standard practice and include:-

1. Visual inspection.
2. Metallography.
3. α -counting for surface and near surface contamination.
4. Acid leaching.
5. Density measurements on both kernel and coated particle.
6. Microradiography.
7. X-ray powder and chemical analysis.
8. Xenon emission.

9. High temperature treatments followed by repeat of (3) and (4).

10. Crushing strength.

2.2 Types of Irradiation Tests

Although most of the tests described in this paper have been carried out under static conditions in sealed capsules, some results from the Pluto Loop and Studsvik purged capsules are also included. The irradiation conditions and the type of fuel used in each test are summarised in Table 1.

The AERE P1 and DY irradiations were carried out on unsupported particles located in small diameter holes drilled longitudinally in a block of graphite surrounding a central thermocouple. Individual capsules were used to permit post-irradiation measurements of fission gas release. Standard AERE light water cooled rigs for 4V holes [10] were used for the irradiations.

The design of the rigs and loops employed by the Dragon Project have been described in detail elsewhere [11, 12], and are, therefore, only briefly described below.

The HPD (high power density) rigs were developed for the initial irradiation evaluation of different types of particle. All the fuel particles in HPD2-4 were incorporated into twelve compacts, 0.4 in. dia. x 0.5 in. in length. Modifications have now been made (HPD5 and following) to irradiate some unsupported particles in addition. As all the compacts are contained in one capsule no gas release data can be obtained if any variables are included. The rigs are irradiated in an in-core position in the Riso reactor.

The Pluto loop is capable of irradiating a 3 ft length of a Dragon fuel element under realistic conditions of rating, temperature and coolant flow. Eighteen full size Dragon compacts are irradiated in a low permeability graphite tube, the tube being cooled externally by helium. A purge stream flows down the central hole of the fuel inserts to sweep out the gaseous and volatile fission products for collection and subsequent measurement in special traps.

The Studsvik purged capsules are capable of testing specimens of the same type as the HPD rig sample and independently measuring fission gas and volatile fission product emission. The temperature of the sample can be varied by changing the carrier gas from helium to neon.

FISSION PRODUCT RELEASE RESULTS

Post-irradiation fission product gas release measurements were obtained on all the DY series and the graphite components on two capsules (DY3 and 7) are also being analysed for solid fission products by Fission Product Technology Group, AERE. In-pile fission gas release data are available for Pluto Loop IIIA and Studsvik I charges, brief summaries of which are included in this report so that comparisons with microscopic observations can be made. Work is still in progress on the radiochemical analysis of the loop components to obtain the solid fission product release data; this will all be reported in detail elsewhere.

Table 1

Summary of Fuel Charge Details

Details of Fuel Fabrication, Coating, Pre-Irradiation Assessment, and Irradiation Conditions are Given for the Various Charges in Tables 4-8.

Charge	Kernel Type	Theoretical Density %	Coating Type	Irradiation Temperature °C	Burn-up			Objective of Experiment
					% FIFA*	% FIMA*	Fission/fuel kernel cm ³	
P1 DY	Sintered UC ₂ Sintered UC ₂	70 70	Laminar PyC 2 stage Laminar PyC 2 stage	800 920-1320	9 3.1-7.3	9 3.1-7.3	1.8×10^{21} 5.7×10^{20} to 1.35×10^{21}	Initial high burn-up tests on AERE fabricated particles; to investigate the temperature dependence and mechanisms of failure.
HPD2	Sintered UC ₂	70	Laminar PyC 2 stage	1250-1500	6.5-7.5	6.5-7.5	$1.20-1.40 \times 10^{21}$	
HPD4	Sintered 5:1 (Th,U)C ₂ Melted 5:1 (Th,U)C ₂ Melted 5:1 (Zr,U)C	50 80* 94	Laminar PyC/SiC/Laminar PyC	1150-1400	12-16	2-2.7	3×10^{20} 4.3×10^{20} 1×10^{21}	Radiation behaviour of triplex coatings. Comparison of sintered versus melted particles.
HPD5	Sintered 5:1 (Zr,U)C	65	1st Coating interrupted laminar 2nd Coating Types 1 and 2 - Columnar 3 and 4 - Laminar	1200-1750	12-16	2-2.7	7×10^{20}	Effect of coating variables and temperature on one type of kernel.
Pluto Loop IIIA (PL)	Sintered UC ₂	50	Laminar PyC 2/3 stages	700-1200	7-14	7-14	9×10^{20} to 1.8×10^{21}	Initial Pluto Loop test on coated particles fabricated by Dragon. Very high burn-ups.
Studsvik I	Sintered 10:1 (Th,U)C ₂ Melted 10:1 (Th,U)C ₂	82 94	Laminar PyC/SiC/Laminar PyC	800-1270	18	1.6	2.9×10^{20} 3.4×10^{20}	Complementary to HPD4. Study fission product release from triplex coatings with fairly realistic (Th,U)C ₂ kernels. Comparison also melted versus sintered kernels.

*% Fifa = % fissions per initial fissile atom

% Fima = % fissions per initial metal atom.

(a) Post-irradiation Measurements for Capsule Tests

	Temperature °C	Burn-up % Fima	Fractional Release Kr-85 *
DY1	1250	7.1	1×10^{-4}
3	1300	7.3	2×10^{-5}
5	925	6.6	2×10^{-5}
7	1275	4.3	5×10^{-6}
9	1000	3.3	-

*Limit of accuracy is low for the lower releases; 5×10^{-6} represents lower limit.

(b) In-pile Gas Release from Pluto IIIA

$$\text{Fractional release} = \frac{\text{release rate}}{\text{birth rate}} \left(\frac{R}{B} \right)$$

	Kr-87 78m	Kr-88 2.77 h	Kr-85m 4.4 h	Xe-135 9.2 h	Xe-133 5.27 d
At start-up		2.7×10^{-4}	2.3×10^{-4}	9.2×10^{-5}	2.7×10^{-4}
Final	3.4×10^{-4}	4.5×10^{-4}	2.2×10^{-4}	1.7×10^{-4}	4.2×10^{-3}

(c) In-pile Gas Release from Studsvik 1

A series of plots of average $\frac{R}{B}$ values versus half-lives of the fission gas isotopes for the three loops are given in Fig. 32.

The higher release from loop B agrees with the microscopic observations that some particle coatings were completely destroyed from reaction with the thermocouple and hence only Loops A and C represent a true indication of the properties of these particles. For comparison the data obtained by ORNL [13] from duplex pyrocarbon coated particles irradiated at 800°C to a burn-up of 15% are plotted.

4. RESULTS OF MICROSCOPIC EXAMINATION

4.1 Fuel Kernels

4.1.1 UC_2 Kernels

Fully enriched, sintered UC_2 kernels were used as fuel for the P1, DY, HPD2 and Pluto Loop IIIA charges. Irradiation conditions covered the temperature range $700\text{--}1500^{\circ}\text{C}$ and burn-up in the range 3-14% Fima.

4.1.1.1 Phases in Fuel Kernel

The fuel kernels, as fabricated, consisted of UC_2 with a small amount of UC. Those of the DY series in addition contained small amounts of discrete graphite particles. During the initial coating stages some pyrocarbon was deposited within the pores and as a thin surface layer on the kernels (Fig. 1).

Three distinct types of phase distribution were observed after irradiation:-

- (i) The majority of the kernels, irrespective of irradiation temperature in range $800-1300^\circ C$, viz., P1 and PL IIIA/2 ($800^\circ C$), DY3 ($1300^\circ C$), DY7 ($1275^\circ C$) and PL IIIA/9 ($1150^\circ C$), consisted of a white carbide matrix containing a dispersed grey phase which was also present as a continuous surface layer (Fig. 2, 3 and 6). The grey phase was not attacked by the normal carbide etchant ($1:1:1 HNO_3:HAc:H_2O$) and showed elastic behaviour when subjected to microhardness tests. This behaviour suggests that the grey phase is a form of carbon. In all cases densification has occurred, but whilst in the low temperature irradiated kernels (P1 and PL IIIA/2) no voidage existed within the kernel, at higher temperatures some voidage was present within the carbon phase (described in next section).
- (ii) A much coarser distribution of carbon was found in PL IIIA/5 ($1000^\circ C$) and PL IIIA/1 ($700^\circ C$), having appeared to have nucleated on the sites of cracks or large pores present in the original kernel (Figs. 4, 5 and 10).
- (iii) The sole exceptions to this total redistribution of carbon were a small proportion of the particles from capsules DY1 and 5, where contrary to all the other observations, the kernels remained unsintered and some of the original discrete graphite particles present in the unirradiated material were still observable.

In summary, no pattern of temperature and/or burn-up effects with the phase distribution present in irradiated fuel kernels has been obtained.

The carbide phase in PL IIIA/5 was sufficiently coarse to obtain an estimate of the microhardness as 740 ± 40 DPN (cf., UC (as cast) 700 DPN and UC_2 (as cast) 500 DPN [14]). Overall carbide plus carbon microhardness measurements on fuel kernels from the No. 2 and 9 compacts were 400 and 300 DPN respectively. The response of the carbide phase to

the nitric/acetic acid etchant showed that the particles irradiated at 700-900°C darkened in two minutes while all the others darkened in about twenty seconds. This etch when used on unirradiated fuel darkens the UC after twenty seconds and the UC₂ after 1-2 minutes. This suggests, but does not prove, that the UC₂ has transformed to either U₂C₃ or UC in the higher temperature irradiations; what has not been established however, is the effect of varying concentrations of fission products, produced during burn-up in the range 3-14%, on the etching characteristics of the carbides.

On the other hand, preliminary results from X-ray diffraction measurements on particles from the DY7 capsule have shown that both UC₂ and UC are still present.

4.1.1.2 Sintering and Swelling

The most obvious effect observed in the majority of irradiated UC₂ kernels is the virtual absence of porosity within them compared with the as-fabricated kernels which contained upwards of 30% porosity (cf., Fig. 1 with Fig. 2). Densification occurs over the whole temperature range covered by these tests, but it is most pronounced at the lower temperature, i.e., 700-800°C (P1 and PL IIIA/2). The microstructure shows a fine dispersion of dense carbon in carbide (Fig. 6).

At high temperatures the effect does not appear so marked when the kernels are viewed at low magnifications (X100), but at higher magnifications (X1000) the carbide phase is seen to be dense and the porosity present occurs within the carbon phase. This is a general observation with these particles.

Further evidence that the fuel kernel has shrunk is that either a gap is observed between kernel and coating (Fig. 2), in contrast to the closer contact observed in unirradiated particles, or, where a whole inner layer is observed to have contracted away from the outer coating, the fuel kernel is still confined within the inner coating (Fig. 3).

In most cases there is little or no migration of additional carbon into the kernel. Measurements of the thickness of the pre-coat pyrocarbon adhering to the kernel normally remains essentially unchanged, although there are some exceptions to this latter observation which are discussed later.

That the sintering is in some way irradiation-induced was shown by the fact that an out-of-pile anneal of some DY particles in the temperature range 1150-1350°C for the full irradiation period of 40 days caused no microstructural change.

Two exceptions to this form of behaviour have been observed:-

- (a) A small proportion ($\sim 10\%$) of the total number of particles in DY1 and 5 did not sinter appreciably. In all cases where this occurred there was pronounced diffusion of the fuel phase into the coating (Fig. 8).
- (b) Particles in HPD2 and a further small percentage of DY5 particles, showed a less marked sintering effect; in this case both diffusion of carbon into the fuel kernel in addition to the outward migration of the fuel (Fig. 9) had occurred. These points are discussed further in the section on pyrocarbon coatings.

The sintering and densification is at least partly offset by swelling of the fuel, which will consist of contributions from the solid fission products situated either within the carbide crystal lattice or at grain boundaries, and from the gaseous fission products, the effect of which will depend on the way the gas bubbles are nucleated. The observed effect of swelling in the particles is to cause local expansion of the kernel into voidage provided by cracks in the inner layer(s) of the pyrocarbon coating (Figs. 2 and 20). At the test temperatures UC_2 appears to be able to deform readily without cracking.

It has not been possible, however, to establish any idea of the volume increases produced because of the sintering effect and the range of kernel sizes, and in any case, taking one section across a kernel may also present a non-typical condition. Similarly, it is impossible to give any indication of the burn-up and temperature dependence of swelling except that it is observed at burn-ups as low as 3% of total metal atoms and at temperatures as low as $800^{\circ}C$.

Fission gas bubbles are not normally resolvable within the carbide phase under the optical microscope. There is evidence of a fine precipitate in the carbide phase in some instances, e.g., Pluto Loop IIIA/5 (Fig. 10) which could be interpreted as bubbles, but this question will need to be resolved by electron microscopy.

One exception to the absence of gas bubbles is the P1 particles. Although no bubbles were observed within the fuel in the intact particles, which were similar to those shown in Fig. 2, all the failed particles contained bubbles ranging in size up to 25μ in diameter (Fig. 11). The appearance of the coating suggested that failure was due to excessive internal pressure, so it seems reasonable to postulate that the restraint provided by the coating up to the point of failure was sufficient to restrain the gaseous swelling.

The P1 particles were irradiated at only 800°C , and hence it is likely that the gas retention within the kernel was higher than for equivalent particles irradiated at higher temperatures. In contrast to the P1 behaviour no such difference in the swelling of failed and intact particles has been observed in the other series, even in PL IIIA/2.

4.1.2 $(\text{Th},\text{U})\text{C}_2$ Kernels

The melted kernels, prepared by plasma arc melting of sintered spheroids, had a coarse striated type of structure and appeared to be monocrystalline before irradiation. Many of the 5:1 $(\text{Th},\text{U})\text{C}_2$ kernels had become polycrystalline, however, after irradiation at 1400°C followed by annealing at 1500°C for two hours. The recrystallisation appeared to proceed from the edges towards the centre of the particles and often three zones were visible (Fig. 12): a completely recrystallised, light-coloured outer zone, a dark irregular intermediate zone, and an inner zone where the original structure is still weakly visible. Accary [15] has suggested that the recrystallisation may be due to a phase transformation of ThC_2 believed to be reversible and to occur at about 1300°C , but which is not yet well authenticated. Similar kernels irradiated at 1300°C did not transform but retained the unirradiated structure, and many exhibited cracking along the crystallographic planes (Fig. 13). The cracks frequently extended through the particle coating. Similar effects were noticed during the coating of these kernels, and are probably caused by the thermal release of stresses locked in the kernel during the rapid cooling following melting in the plasma arc.

The results from Studsvik I on melted kernels of 10:1 $(\text{Th},\text{U})\text{C}_2$ seems to be at variance with those from HPD4 reported above, since kernels irradiated at a maximum temperature of only 1100°C had completely recrystallised. Whilst it is possible that the change in Th:U ratio from 5:1 to 10:1 together with an increase in free carbon in the fuel from 0.2 w/o to 1.0 w/o had affected the transformation temperature, it is also possible that the recorded temperatures in Studsvik I were in error, reading in fact several hundred degrees low in all the capsules, since the platinum sheathed thermocouple in B (nominal temperature 1270°C) had reacted with both the graphite matrix and coatings whereas such thermocouples normally withstand temperatures of 1500°C for long periods without any reaction occurring.

Both the 5:1 and 10:1 $(\text{Th},\text{U})\text{C}_2$ sintered kernels showed little change on irradiation at 1375 and 1150°C respectively, though a greater degree of sintering was observed at the higher temperature (Fig. 14).

4.1.3 $(\text{Zr},\text{U})\text{C}$ Kernels

The melted 5:1 $(\text{Zr},\text{U})\text{C}$ kernels in HPD4, although prepared by the same technique as the $(\text{Th},\text{U})\text{C}_2$ kernels, were polycrystalline. They withstood irradiation at 1400°C without showing any signs of cracking (Fig. 31).

Similarly, the sintered 5:1 (Zr,U)C kernels from HPD5 showed little change after irradiation at a series of temperatures between 1300-1700°C (Figs. 27-30).

4.2 Coatings and Interactions between Fuel and Coating

4.2.1 Pyrocarbon Coatings

Two main types of coating have been investigated:-

- (a) Double or triple layers of laminar type (P1, DY, HPD2 and Pluto Loop IIIA). Thickness range: 62-78 μ .
- (b) An initial layer (25 μ) of laminar pyrocarbon containing interruptions, followed by a thicker layer of either laminar or columnar type pyrocarbon (HPD5). Thickness range: 70-115 μ .

A summary of the results with these two types of coating and the probable causes of the observed failures is presented in Table 2.

4.2.1.1 Diffusional Effects

Three apparently different forms of diffusion of fuel into the pyrocarbon have been observed. One is a straightforward phenomenon occurring only at high temperatures whilst the others appear to be associated with lower temperatures.

Thermal annealing of unirradiated particles will produce quite appreciable migration of UC₂ fuel into the pyrocarbon coating at 2000°C after only three hours, and complete penetration at 2200°C (Fig. 15). In terms of long term in-reactor behaviour, based purely on the out-of-pile data, temperatures in excess of 1700-1800°C are likely to show evidence of this phenomena. Particles irradiated in the HPD3 test showed quite clearly that at temperatures in the region of 1900°C, complete penetration of the coating occurred. The direction of migration was, however, random in contrast to the "amoeba" effect reported by General Atomic [16], in which migration toward the higher temperature was observed. Post-irradiation annealing at 1800°C for 1 h of the PL IIIA/7 compact showed local evidence of fuel migration into the coating to a depth of ~5 μ (Fig. 16). In these high temperature treatments counter diffusion of carbon into the fuel is also observed.

A somewhat similar phenomenon was observed in a small percentage (~10%) of the particles in both the DY1 and 5 capsules. This was surprising in view of their low operating temperatures, i.e., 1270° and 920°C. Contrary to the normal behaviour, where no diffusion of the fuel into the coating had taken place, neither sintering nor densification occurred (Fig. 8 and 17a). The diffusion zone extended 20-40 μ into the coating and was more uniform than the high temperature type. Further major differences

Table 2
Summary of Failures on Pyrocarbon Coated Particles

Charge	Kernel Type	Theoretical Density %	Irradiation Temperature °C	Burn-up % Fima	Coating Type, Deposition Temperature and Thickness	Failed Coatings (Estimated microscopically) %	Probable Cause of Failure
P4	Sintered UC ₂	70	900	9	Laminar 2 stage/1830°C/69μ	5	Coating fracture due to fuel swelling and possibly excessive internal pressure.
DY 1,2 3,4 5,6	Sintered UC ₂	70	1250 1300 925	7.1 7.3 6.6	Laminar 2 stage/1650°C/62μ	0 0 1	External corrosion coupled with diffusion of fuel into coating.
7,8 9,10	Sintered UC ₂	70	1275 1000	4.3 3.3		0 0	
HPD2/3A	Sintered UC ₂	70	1300-1500	7.5	Laminar 2 stage/1650°C/62μ	>50	Spearhead penetration together with counter diffusion of coating and fuel material. Suspected that irradiation temperature was higher than estimated by calculation.
/6A	Sintered UC ₂	70	1250-1450	6.5		>50	
Pluto Loop IIIA-2 -5 -9	Sintered UC ₂	50	800 1000 1150	8 12 14	1st stage Laminar/1350°C 2nd stage Laminar/1600°C 3rd stage Laminar/1400°C	10 20 50	Spearhead attack. Spearhead attack coupled with external corrosion.
HPD5/2A 4B 6B	Sintered 5:1 (Zr,U)C	65	Type C200 1620 1450 1310	2-2.6	1st coat Interrupted laminar/1600°C/20-25μ 2nd coat Columnar/1800°C/53μ	0 0 0	
1A	Sintered 5:1 (Zr,U)C	65	Type C201 1300		1st coat Interrupted laminar/1600°C/20-25μ	12	Brittle radial cracks following spearhead attack to depth of 20-30μ into coating. Some failures in centre of compact due to reaction with platinum thermocouple. Spearhead cracks extending 50-75μ into coating.
3A	Sintered 5:1 (Zr,U)C	65	1660	2-2.6	2nd coat Columnar/1600°C/50μ	0	
5A	Sintered 5:1 (Zr,U)C	65	1375			75	
HPD5/4B 3B 5B	Sintered 5:1 (Zr,U)C	65	Type C202 1300 1660 1375	2-2.6	1st coat Interrupted laminar/1600°C/20-25μ 2nd coat Laminar/1600°C/40μ	0 (50% around edge) 0	Some failures in centre of compact due to reaction with platinum thermocouple. Wide radial cracks appearance of relief of high internal pressure.
2A 4A 6A	Sintered 5:1 (Zr,U)C	65	Type C203 1620 1450 1310	2-2.6	1st coat Interrupted laminar/1600°C/20-25μ 2nd coat Laminar/1450°C/95μ	0 0 75	
							Thin hairline cracks in coating possibly associated with stress and corrosion.

Table 3
Summary of Failures on Triplex Pyrocarbon/SiC/Pyrocarbon Coated Particles

Charge	Kernel Type	Theoretical Density %	Irradiation Temperature °C	Burn-up % Fima	Coating Type, Deposition Temperature and Thickness	Failed Coatings (Estimated microscopically) %	Probable Cause of Failure
HPD4/2A 3A	Melted 5:1 (Th,U)C ₂	80+	1350 1400; Annealed 1500 2 h	~2.7 ~2.7	1st coat Laminar PyC/1450°C/8μ 2nd coat SiC/1600°C/41μ 3rd coat Laminar PyC/1700°C/32μ	90 10	Brittle cracks, extending through all three coating layers, associated with severe kernel cracks. Brittle cracks in SiC coat induced attendant cracks in PyC.
3B	Melted 5:1 (Zr,U)C	94	1400	~2.7	1st coat Laminar PyC/1450°C/22μ 2nd coat SiC/1640°C/22μ 3rd coat Laminar PyC/1720°C/30μ	0	
4B	Sintered 5:1 (Th,U)C ₂	50	1375	~2.7	1st coat Laminar PyC/1460°C/8μ 2nd coat SiC/1700°C/60μ 3rd coat Laminar PyC/1800°C/40μ	0	
Studsvik I A1	Sintered 10:1 (Th,U)C ₂	82	900-1150*	1.2	1st coat Laminar PyC/1340°C/5μ 2nd coat SiC/1600°C/76μ 3rd coat Laminar PyC/1700°C/40μ	0	
B1 C1	Melted 10:1 (Th,U)C ₂	94	970-1270* 850-1100*	1.15 1.6	1st coat Laminar PyC/1380°C/5μ 2nd coat SiC/1600°C/64μ 3rd coat Laminar PyC/1700°C/44μ	0 0	Failure of some particles associated with corrosion from platinum thermocouple.

*These temperatures are thought to be too low.

from the high temperature effect were:-

- (1) Particles of fuel were only resolvable under the microscope at the front of the diffusion zone. The pyrocarbon through which the fuel had passed appeared in a very porous state (Fig. 8).
- (2) There appeared to be no diffusion of carbon into the fuel kernel.

A further marked effect, in contrast to the remainder of the particles in the two capsules, was the almost complete absence of spearhead attack in the coating when diffusion of the fuel occurred.

A second form of low temperature migration has been observed in nearly all the particles examined in the HPD2 compacts and in a few isolated particles in DY5 (Fig. 9). These kernels were from the same batch and although not coated together were coated under nominally identical conditions in two successive runs. This type of diffusion is two way, both carbon and fuel migrating. In all cases where this type of behaviour was observed a large amount of the inner of the two coatings appears to have been corroded away, and similarly the outer coatings if not breached completely were so badly corroded (usually in a laminar form which resulted in a fibrous appearance) that they would be considered as failed coatings. It is highly likely in these cases that a breach of the coating would be observed if a complete 3-dimensional picture was obtained. Almost all the HPD2 particles were badly attacked in this way, whereas only a few in DY5 behaved in this manner, and these were the only failed particles found in the DY series.

This type of behaviour can therefore be associated with particles that have failed by an external corrosive attack which in laminar pyrocarbon causes lamination. In fact, whereas the DY capsules were given a degassing treatment before sealing, no such treatment was given to the HPD2 compacts, and these are likely to contain moisture in addition to other adsorbed gases. It is not clear how the few DY particles were attacked.

In the Pluto Loop IIIA, which was the only other instance of a large proportion of failure in pyrocarbon- UC_2 particles, the kernels in both failed and intact particles normally appeared the same. Corrosive attack was observed on the outer surface of some of the pyrocarbon coatings, but only in a relatively few instances, mainly in the No. 9 compact, did this cause severe lamination of the outer coating (Fig. 18). In these cases some carbon migration

into the fuel had occurred but not to the same degree as in the other instances.

4.2.1.2 Spearhead Attack and Shrinkage of Pyrocarbon

"Spearhead attack," which in section normally appears as V-shaped voids originating at the fuel coating interface and extending into the pyrocarbon, is observed in most of the specimens. A 'three-dimensional' picture obtained by sectioning a particle through the fission fragment recoil layer shows that the path formed by the void is not circumferential but has a fairly characteristic 'X' shape (Fig. 19). "Primary spearheads," regardless of burn-up and temperature, are remarkably uniform in their depth of attack and normally penetrate 20-25 μ into the coating (Fig. 20). The fission fragment recoil range in fully dense graphite is 13.6 μ and in pyrocarbon having a density of 1.5 g/cm³ it is 20 μ . No correlation has been found between the volume of spearhead voidage and temperature, burn-up, or temperature of deposition (hence density of pyrocarbon), because in the random cross sections taken there is too much variation even within a batch of particles irradiated under the same conditions.

Coating failures are very often the result of continuing growth of the primary spearhead through the coating. It was encouraging to find, therefore, that in the DY series, apart from the corrosion effects noted previously, no failed particles were observed. These particles had a double laminar coating, and the spearheads rarely penetrated further than a few microns beyond the interface between the two layers; the tip of the spearhead tended to turn circumferentially either before or on meeting the interface. The interface was introduced into this batch to ensure that the outer coating was free from contamination; this was achieved by removing the particles from the fluidised bed after the first coat and leaching before returning for the application of the second one. The ability of an interruption to apparently halt or at least delay the continued growth of primary spearheads had also been observed in ORNL particles having a duplex structure of the laminar/columnar type tested at ORNL [17].

The microscopic observation that the spearhead was a void, and not a heavily damaged region of pyrocarbon which was removed on polishing, was confirmed by microradiography carried out by the technique described by Sharpe [18], (Fig. 21). Microradiographs also confirmed the shape of the spearhead and showed that these were not circumferential cracks.

In some particles (DY particularly) the pyrocarbon damaged by recoil of fission fragments is clearly visible as a darker band when viewed under incident white light (Fig. 3). This region under polarised light polarises

very strongly compared with the remainder of the coating which is only weakly responsive (Figs. 22a and b), and suggests a degree of ordering or possible graphitisation in this layer adjacent to the kernel.

In the DY1 and 5 particles in which the diffusion of fuel into the kernel was observed, a shell 20 μ thick immediately outside the diffusion zone responded to polarised light in addition to the pyrocarbon through which it had passed (Figs. 17a and b). As noted previously, no spearhead attack was present in these particles.

Although the coatings of the Pluto Loop IIIA particles were actually composed of 2 or 3 layers, due to variations in temperature conditions during coating, these did not produce interruptions in the same sense as in the DY series. In nearly all cases failures were due to the growth of the primary spearheads until eventually the whole coating was penetrated (Fig. 7) though in some cases the effective path was reduced by external corrosion thinning the coating. The percentage of failed particles ranged from 10% for compact No. 2 to 50% for No. 9.

The HPD5 series was prepared to test further the effectiveness of interruptions in the coating in preventing the growth of primary spearheads. The first coat for all the particles, totalling 20-25 μ and deposited at 1600°C, contained three thin layers of laminar pyrocarbon interrupted by two thin columnar layers; the interruptions were produced by altering the partial pressure of methane in the fluidised bed. Four different types of second coating were then applied, viz., columnar coatings deposited at 1600°C (C201) and 1300°C (C200) and laminar coatings at 1450°C (C203) and 1600°C (C202), (Figs. 23-26).

Microscopic examination of this series has shown that only one type of coating failed as a result of growth of spearheads, viz., the 1600°C columnar (C201) irradiated at 1375°C (Fig. 27). One particular feature was that the penetration of the spearheads was less severe at the highest irradiation temperature (1660°C) (Fig. 28). In the other three types the interrupted laminar coatings were basically successful in that the furthest penetration into the outer coating was limited to 5 μ , and there was no sharp tip to the spear which would tend to propagate a crack through internal pressure. A large number of failed particles were, however, observed in both the C202 and C203 types, in one compact out of the total of three of each type that were irradiated, but the causes for failure appear different, and are discussed later. The irradiation temperatures of the compacts containing the failed particles were 1375 and 1310°C respectively.

Since it has been shown by microradiography that the spearheads are voids and since it has also been argued

that mass transfer or diffusion of the pyrocarbon has not occurred except at the very high temperatures, the inner section of the coating must be shrinking. Further evidence of this is afforded by the frequent observation that the whole of the inner coating (particularly in the DY series) (Fig. 3), or a thin layer within it (Fig. 22a) separates from the remainder of the outer coating leaving a gap. The thickness of this thin layer is approximately equal to the fission fragment recoil depth. This separation is also seen in microradiographs (Fig. 21). In extreme cases where the whole of the inner coating apparently contracted intact without formation of spearheads, a gap of $5-10\mu$ has opened up between inner and outer coating (Fig. 3).

Further evidence of the ability of pyrocarbon to deform is obtained from the observation that there is a greater separation locally between the inner and second layer (Fig. 9) adjacent to a spearhead crack which has not quite penetrated the inner layer.

The ability of pyrocarbon to deform markedly is again shown in those particles that had failed in the P1 series of tests. The pyrocarbon adjacent to the crack curls in toward the fuel kernel indicating the relief of large internal stresses upon fracture (Fig. 11). Similar effects have been observed by the BMI [23] and ORNL [19] workers.

4.2.1.3 Other Cracking Phenomena

(a) Wide Radial Cracks

These occur as wide parallel sided cracks running through the whole thickness of the coating (Fig. 29). One to three such cracks are observed in a cross section, usually regularly spaced around the circumference. Failure must have taken place in a brittle manner since no local deformation was noted in the adjacent coating material. This type of failure was observed in 90% of particles in one compact in HPD5 charge (C202) though the penetration of inner coating was of the usual spearhead type.

The mode of failure suggests bursting under an internal pressure. Notwithstanding the fact that the particles were retained by a matrix, some of the cracks had opened up to widths of 50μ or more.

(b) Hairline Cracks

These have been observed only in two instances in laminar coatings from the HPD5 series. In one compact containing the low temperature laminar coating (C203) 75% of the coatings in the field observed contained fine cracks originating at the outside surface (Fig. 30). They were randomly orientated with respect to the compact and varied in form in the particles, some cracks being

approximately radial, other cracks being wholly within the coating. Initially it was thought that the polished section had been taken too close to the cut face, but a second section taken 0.050 in further in from the cut face showed exactly the same phenomena. The other instance where particles exhibited this behaviour was in the high temperature compact (1660°C) containing the (C202 type) high temperature laminar coating. This compact initially surrounded a centrally placed platinum sheathed thermocouple (Pt-0.1% Mo, Pt-5% Mo) which melted during irradiation. The centre zone of particles was badly corroded by platinum diffusion into the compact, but immediately adjacent to these was a narrow zone of particles that exhibited hairline cracks in the coating. In the outer zone no cracked particles were seen. It seems, therefore, that this cracking could be initiated by stress and impurities, though no corrosion of the carbon coating was observed.

4.2.2 Triplex Coatings (Pyrocarbon/Silicon Carbide/Pyrocarbon)

Triplex coatings on both melted and sintered $(\text{Th},\text{U})\text{C}_2$ and melted $(\text{Zr},\text{U})\text{C}$ kernels have been tested in the HPD4 and Studsvik I charges. The coatings consisted of an inner laminar pyrocarbon layer of $0\text{--}20\mu$, an intermediate silicon carbide layer of $30\text{--}60\mu$, and an outer laminar pyrocarbon layer $\sim 30\mu$ thick.

The inner pyrocarbon layer was invariably heavily damaged by spearhead attack, but no evidence for the growth of spearheads into the silicon carbide layer could be found. No damage could even be detected in some sintered 5:1 $(\text{Th},\text{U})\text{C}_2$ particles (Fig. 14) where the inner pyrocarbon layer was so thin that the silicon carbide was effectively bonded directly to the kernel.

Cracking in the silicon carbide layer occurred in some particles with both types of melted kernel. Gross cracking of all three coating layers occurred with the 5:1 $(\text{Th},\text{U})\text{C}_2$ particles when the kernels themselves shattered during irradiation (Fig. 13). Where recrystallisation occurred, both in HPD4 (Fig. 12) and in Studsvik I with 10:1 $(\text{Th},\text{U})\text{C}_2$, the SiC layer remained intact.

The melted 5:1 $(\text{Zr},\text{U})\text{C}$ kernels did not crack, but their SiC coating had cracked radially in a brittle manner in a few particles, the cracks often extending from the tips of spearheads in the inner pyrocarbon coating (Fig. 31). The outer pyrocarbon coatings remained undamaged.

Post-irradiation annealing was carried out on two compacts from the HPD4 charge in order to assess whether heating above the irradiation temperature would cause additional failures. The inserts were annealed at 1500°C in a helium purge stream, the Xe-133 release being measured. It has been established that, despite the common containment of all twelve inserts, the Xe-133 absorbed in the matrix is quickly released when the capsule is opened and the contamination remaining is only a fraction of that contained in one particle.

The particles with melted $(\text{Th},\text{U})\text{C}_2$ kernels irradiated at 1400°C gave a small steady release of fission gas during the post-irradiation heating to temperatures of 800 - 900°C , corresponding to the Xe-133 contained in 30 particles. Little further release was observed on annealing at 1500°C for two hours, indicating that no failures had been induced by heating. Microscopic observations confirmed that some broken particles had been present. The Xe-133 release from the melted $(\text{Zr},\text{U/C})$ particles irradiated at 1325°C was only a fraction of that contained in one particle and no broken particles were observed on subsequent examination, again indicating that heating of this type of particle to 1500°C has little effect.

5. DISCUSSION ON THE FACTORS AFFECTING PARTICLE INTEGRITY

If a coating is to impede the release of fission products from the fuel kernel it is necessary that some portion of it remains essentially "undamaged" throughout the whole of its life. The minimum thickness required is a uniform layer greater than the fission fragment recoil range (20 - 25μ) from the point of furthest advancement either of the fuel, or of a spearhead, into the coating. The term "undamaged" must imply that neither its diffusional nor mechanical properties are seriously affected. Conversely, failure of a coating can be defined as either a crack, a spearhead, or a diffusion zone extending to less than 25μ from the outer coating surface.

Many factors, either singly or in combination, could cause premature failure of the coating. In the following discussion those which are considered to be the more important are high-lighted.

5.1 Volume Changes in the Kernel

The overall volume change that occurs in a sintered fuel kernel during irradiation is caused by two opposing processes, sintering and swelling.

The sintering behaviour of UC_2 under irradiation is marked even at the lowest irradiation temperatures (800°C) and burn-ups (3%) that have been covered in these tests. This effect has to be viewed against the background that the fuel kernels were initially sintered at 1600°C and that annealing of particles from the DY series for 40 days at 1350°C produced no observable effect. $(\text{Th},\text{U})\text{C}_2$ and $(\text{Zr},\text{U})\text{C}$ kernels do not appear to show such a marked change, but precise comparative experiments have not been carried out.

As yet there is no information regarding the minimum temperature or dose required to produce a noticeable densification; experiments to investigate these factors are underway.

This densification during irradiation appears to have a very beneficial effect on the fission product retentivity of the kernel compared with the as fabricated material. At the same time the use of porous kernels provides voidage for swelling due to accumulation of fission products.

The manner in which swelling occurs locally into available voidage provided by spearhead attack indicates that UC_2 deforms readily under irradiation at temperatures as low as 800°C , whilst the unirradiated material does not show marked plasticity until 1100°C [14]. As the hardness of the carbide phase measured on a kernel from Pluto Loop IIIA/5 indicated a similar value to that reported for as cast UC_2 , the observed plasticity

appears to be an irradiation induced phenomenon similar to that observed in UO_2 after high burn-ups [8].

No swelling effects were observed in the $(\text{Th},\text{U})\text{C}_2$ and $(\text{Zr},\text{U})\text{C}$ sintered kernels, but as these had not densified to the same extent as the UC_2 kernels, any swelling would have probably occurred into the internal porosity and hence not be so noticeable. The burn-up levels achieved so far are, however, lower than those attained in the UC_2 kernels. The impression given in the HPD5 series containing the sintered $(\text{Zr},\text{U})\text{C}$ kernels is that failure in the three types in the range $1300-1400^\circ\text{C}$ generally appeared to be associated with slightly lower density kernels. It is, however, not possible to determine whether this pre-existed before irradiation, or if the decrease in density occurred after the coating had fractured.

No swelling was observed in the melted $(\text{Th},\text{U})\text{C}_2$ or $(\text{Zr},\text{U})\text{C}$ particles, though the maximum burn-up attained is only 2.7% fima. The thorium containing particles either remained monocrystalline and cracked, or underwent a phase transformation which tended to mask any swelling effects. High burn-ups (30% fima) have been achieved at irradiation temperatures below 950°C with melted UC_2 particles at ORNL [19], and though the swelling has been quite high it was not sufficient to cause failure of the coating, sufficient voidage apparently being provided by spearhead attack and by the soft carbon layer adhering to the kernel from the fabrication stage.

It is not yet possible to analyse fully the relative merits of melted and sintered particles, as comparable specimens have not been tested to sufficiently high burn-ups. It is apparent that it is necessary to avoid single crystals in the melted particles. With sintered particles it appears that the initial estimate of the voidage necessary was pessimistic, the only evidence of swelling causing failure being in the P1 particles, and further, it does not appear that the assumed higher gas release from sintered particles constitutes a problem in itself. The economic advantage would seem to lie with sintered particles.

5.2 Fission Product Release

Fission gas release results were obtained from the DY static capsules and from the Studsvik purged capsule and Pluto IIIA Loop tests. A reasonable correlation with the number of failed particles observed under microscopical examination was obtained on all except the Pluto Loop results.

In the DY (pyrocarbon coated UC_2) capsules, the low fractional release of Kr-85 measured (10^{-4} to 5×10^{-6}) agreed with the observation that no failed coatings were observed except in DY5 (1% failure). Very low release rates ($\frac{R}{B}$ (Xe-133) = 10^{-6} at $890-950^\circ\text{C}$) were also observed on two of the three purged capsules in the Studsvik I test (PyC-SiC-PyC coated $(\text{Th},\text{U})\text{C}_2$) in which again no failed particles were found. The gas releases showed a marked temperature dependence. The third capsule operating at 1220°C however, gave releases over two orders of magnitude higher

($\frac{R}{B}$ for Xe-133 = 4×10^{-3}). This higher release, however, was mainly attributable to a corrosive effect on the coatings of particles adjacent to the centrally positioned platinum thermocouple.

In neither of the above tests has any attempt been made to estimate the precise number of broken coatings, so that the release rate from a broken or uncoated particle is not known. In both tests surface or near surface contamination of the coating was probably the main contributor to the observed releases.

In the Pluto Loop IIIA test (pyrocarbon coated UC_2) the percentage of failed particles was so high that examination of over 100 particles in each compact was found to give reasonably representative figures, the range being from 50% failure in compact 9 ($1150^\circ C$, 14% fima) to 10% in compact 2, ($800^\circ C$, 8% fima). This high percentage of failures was unexpected as

- (i) the initial release rate ($\frac{R}{B} = 1-3 \times 10^{-4}$ for short-lived gases) corresponded fairly well with that expected from the pre-irradiation measurements of the surface contamination and did not markedly increase throughout the whole period of the irradiation. As the Pluto Loop particles were initially ~50% porous it was, therefore, anticipated that virtually 100% release would occur from a failed particle, but this did not allow for the fact that sintering of the kernel would occur.
- (ii) Previously reported low burn-up tests from General Atomic [20] and ORNL [17], and one high burn-up test from ORNL [21] gave high release values from uncoated fused particles, viz., ORNL test gave $\frac{R}{B} (Xe-133) = 7 \times 10^{-2}$ for up to 4% burn-up at $815^\circ C$.

To explain the results one needs to postulate that the kernels in these broken particles were at least a factor of 5 times more retentive than the ORNL fused particles, even if no account is taken of the higher average operating temperature of the Pluto Loop which obviously gives a pessimistic figure. The only reported instance of a similar discrepancy is from the EMI data [22] on unsupported pyrocarbon UC_2 particles irradiated to 4% burn-up at $1070^\circ C$, in static capsules. The $Xe-133$ releases obtained on post irradiation puncturing of two capsules were 0.52 and 0.75% respectively against failure percentage of 21 and 55% as revealed by leaching tests. These figures were not commented upon, nor was metallographic evidence supplied to support the data obtained by leaching tests.

It is conceivable, though admittedly unlikely, that this form of dense UC_2 produced by sintering in-pile could retain its fission products better than the fused material irradiated by ORNL, even to high burn-ups (14%). If this is the case then its behaviour differs completely from the only other material irradiated to comparable burn-up, viz., UO_2 . Thus:-

- (i) UO_2 suffers a very severe decrease in its powers of fission gas retention above 5% burn-up [8] whilst UC_2 apparently behaves as if its retention powers are increased.
- (ii) UO_2 shows severe gas bubble swelling at burn-ups around 10% even when highly restrained in the form of a cermet, whereas, only in one isolated case (P1) have fission gas bubbles been observed in UC_2 and these were in broken particles. The failed particles in the Pluto Loop specimens did not show any more swelling than the intact ones where restraining forces could

have influenced the growth of bubbles. This absence of gas bubble swelling would seem indicative of low fission gas retention.

(iii) Unlike UO_2 , or any other irradiated fuel for that matter, no burst of fission gas was observed either during in-pile transients or on post-irradiation annealing to $1800^\circ C$.

At this point no obvious explanation exists for this discrepancy between gas release and metallographic appearance. Measurements of the amount of gas remaining in the kernels, and some loop experiments on kernels having only a very thin coating, which according to experience should fail rapidly, should help to resolve this very important practical point.

Excessive internal pressure from fission product gases does not appear, by itself, to have caused failure in any of the particles examined. This is important as the decision to use porous kernels relied on the assumption that the coating could withstand the pressure exerted by released gases and volatiles at the temperature of operation, whilst the lattice swelling in the kernel was not known and could be controlled. Calculations using a pessimistic swelling rate and assuming complete release of gases and volatiles indicated that for a 300μ diameter particle with 100μ coating, 50% voidage would be required for 10% burn-up at $1500^\circ C$ if the maximum stress in the coating, ignoring thermal stresses, should not exceed the tensile strength of pyrocarbon, assumed as 4,600 psi [9].

The small percentage of failures in the DY series has demonstrated that these assumptions were pessimistic; for although these particles only went to 7.3% burn-up at $1300^\circ C$, they only contained 30% porosity and spearhead attack had reduced the effective coating thickness to 37μ .

The low fission gas release results from the triplex coated particles in the Studsvik purged capsules are particularly encouraging in view of the suspicion that the recorded temperatures were low by some hundreds of degrees. If the solid fission product release is found to be as low as the rare gases then these particles represent an extremely promising find.

5.3 Fuel Phase Composition

Some disagreement still exists between workers in the field on the exact conditions under which UC_2 is stable at elevated temperatures [29]. The free energies for the formation of all the three carbides are very close and it appears that small amounts of impurities are able to stabilise certain phases, but so far virtually no work has been done regarding the phase existing after high fission depletion at elevated temperatures.

On etching the fuel kernels the indication was that only the particles irradiated at $700-800^\circ C$ were still dicarbide, whilst after higher temperature irradiation the predominant phase was UC. However, the presence of both phases (as for the unirradiated sample) in the latter was confirmed by X-ray diffraction analysis of particles for DY7.

A lot of questions regarding the phases existing in the kernel remain unanswered at the present and require that the equilibrium diagrams be better defined, particularly for the alloyed carbides, before definite answers can be given.

The presence of fission products such as Zr, Ce and Mo in the fuel, all of which form carbides, could affect both etching and phase equilibria, as at the high burn-ups these constitute amounts greater than 1%.

The composition of the kernels in the HPD series has intentionally included carbon in excess of the stoichiometric composition in order that the kernels operate under saturated carbon conditions. It was thought initially that the attack of the coatings in the HPD2 series resulted from mass transfer of the coating through a gaseous phase to the kernel. Although it is now thought that the spearhead attack does not result from a chemical reaction, it cannot be ruled out that this type of mass transfer process could occur, and may play a part in the growth of spearheads. It is not, however, clear how important the excess carbon has been and separate tests must be performed to define this point.

There also seems to be some evidence for a phase change in the $(\text{Th},\text{U})\text{C}_2$ specimens above 1300°C [15], but more work is required before any conclusions can be made.

In the HPD5 series the kernels were fabricated by sintering a mixture of $\text{UC} + \text{ZrC}$ powders, and were not completely homogeneous. In a subsequent test the route was changed to ensure homogeneity; it will be interesting to compare their behaviour.

5.4 Temperature and Burn-up

The number of failed particles occurring under irradiation for any particular type of kernel and coating will be a complex function of temperature, temperature cycling, burn-up and burn-up rate. Only one test (Pluto Loop IIIA) has really given any indication of the combined effect of temperature plus burn-up on the proportion of failed particles. In the other tests either the degree of burn-up has not been varied over a very wide range (HPD series) or only a few isolated failed particles were observed, as in the DY series.

5.4.1 Temperature Effects

The upper temperature limit for safe operation for UC_2 particles coated with pyrocarbon is fairly well defined. Tests at General Atomic on $(\text{Th},\text{U})\text{C}_2$ [16], and the HPD2 test on UC_2 kernels both showed diffusion of the fuel completely through the coating. The G.A. temperature was estimated at 1900°C while in the HPD2 it was $\sim 1700^\circ\text{C}$; in the G.A. particles the fuel moved toward the higher temperature, but no directionality was noted in the HPD2 samples. However, it is clear that 1700°C represents the upper limit for continuous operation for UC_2 and $(\text{Th},\text{U})\text{C}_2$ particles. No evidence of diffusion was seen in the HPD5 test with $(\text{Zr},\text{U})\text{C}$, the peak temperature of which also approached 1700°C , indicating that the diffusion rate is lower for this material than for the uranium and uranium/thorium dicarbide. Out-of-pile annealing tests on $(\text{Zr},\text{U})\text{C}$ ($\text{Zr:U-235} = 5:1$) at 2000°C confirm this.

At intermediate temperatures the pattern of failures does not present a clear picture. It might be expected that very little of the fission product gases would be retained in the kernel at the

higher temperatures and that a very high internal pressure would result. Neither the type nor overall pattern of failure suggests that fission gas pressure has in itself been a prime factor causing failure and, therefore, other temperature effects must be sought.

The HPD5 series produced the unexpected result that the failure rate of three different types of $(Zr,U)C$ particles was extremely high in the temperature range $1300-1400^{\circ}\text{C}$, yet negligible at $1450-1620^{\circ}\text{C}$. The other rather surprising data was from the BMI results [23] which showed that whereas UC_2 particles coated with 70μ pyrocarbon failed under irradiation in a matter of hours at 100°C , at 1070°C failure did not occur for 5-10 days and resulted from temperature cycling. It was suggested that the low temperature failure was due to stresses locked in during cooling from the coating temperature. The problem was apparently solved by making the coatings thicker, i.e., $>90\mu$, suggesting that locked in stresses were only partly responsible. Although no low temperature irradiations have been performed in this Dragon series, most of the coatings were also about 70μ thick and yet burn-ups up to 8% have been achieved without any failures. This seems to indicate that so many variables are playing a part that at present it is ill-advised to use the information obtained from one type of particle to explain behaviour in another.

Similarly there is no indication that failure rate can be attributed to thermal cycling alone as indicated by the BMI workers. The largest number of thermal cycles occurred in the P1 capsule (47 major cycles) which had 5% failures. The most comparable tests are the DY and HPD2 where irradiation temperature and number of cycles are similar, yet there was no failure in the appropriate capsule in DY compared with over 50% in HPD2.

It has often been stated that heating a particle above the coating temperature will cause thermal stress cracking in the coating. This is not supported by results from either particles of the DY type which have been heated to 2200°C before irradiation, or the Pluto Loop particles which have been heated to 1800°C after 12% burn-up (200°C higher than coating temperature) without additional failure. Similarly in the HPD5 series particles with a laminar coating deposited at 1450°C were irradiated at 1700°C with no failure, yet fine hairline cracks occurred in those irradiated at 1300°C .

5.4.2 Burn-up and Rate of Burn-up

The DY series showed that 8% burn-up could be achieved with pyrocarbon coated UC_2 at temperatures in the range $900-1300^{\circ}\text{C}$ with virtually no coating failure, and ORNL [19] have irradiated particles containing a fused UC_2 kernel with a duplex laminar/columnar pyrocarbon coat to 30% burn-up at temperatures between $800-900^{\circ}\text{C}$ with only 1.5% failure. In the HPD5 series the only particle type which showed 100% intact particles had a duplex coating similar to those tested at ORNL, i.e., outer columnar coat deposited at 1800°C , though the equivalent burn-up in HPD5 was an order of magnitude lower. It appears, therefore, that the burn-ups required in high temperature

power reactors are capable of being achieved, though the conditions required to guarantee 100% success are not well defined.

The surprising conclusion is that burn-up alone does not appear to be one of the major factors affecting particle life. The fact that 30% burn-up has been reached with a very low percentage of failures, albeit at temperatures at the lower end of the temperature range of interest to the Dragon Project, is proof that these high burn-ups are achievable.

Burn-up rate has been varied over a wide range from 0.03% fima/day (comparable to the Dragon rate) to 0.373% fima/day on the undiluted UC_2 kernels in HPD2. Because of the time scale involved in irradiation testing, full burn-up tests have been carried out only on undiluted kernels at accelerated rates while on alloyed kernels the tests so far have only attained 25% of the target burn-ups in spite of thermal flux levels two or three times higher than in the Dragon reactor. Although no obvious effects of burn-up rate have been observed this effect has not yet been studied on one particular type of particle, and one can cite many parameters that may be affected which could perhaps influence the coating integrity.

5.5 Coating Structure

The standard form of pyrocarbon coating tested in these experiments has consisted of two or three layers of the laminar type material. In the HPD5 series the relative properties of columnar and laminar outer coatings were investigated. The obvious disadvantages of the columnar type is that the rate of deposition has to be lower than the laminar type. The particular merit in columnar coatings is that ORNL have reported that the diffusion rate of xenon and krypton is lower than through the laminar type though on the other hand the uranium diffusion rate was faster.

The HPD5 series did not give a clear cut answer on the relative merits of columnar versus laminar coatings. The reasons for failure in some cases are not clear, e.g., a large percentage of failures occurred in a laminar coating deposited at $1600^{\circ}C$ (HPD5/5B) irradiated at similar temperatures and to a much lower burn-up than similar coatings in DY3 and 7. Only one type, having a columnar outer layer deposited at $1600^{\circ}C$, was 100% successful at all irradiation temperatures. This coating is similar to the NCC-AD type irradiated so successfully at ORNL to 30% burn-up, and obviously merits further investigation into both its performance and why under similar conditions the columnar coating deposited at $1600^{\circ}C$ is so inferior. Further tests are already in progress on both laminar and columnar coatings.

The importance of interruptions in the coating in preventing growth of primary spearheads was shown by the DY irradiation series. The pseudo-interruptions introduced in the HPD5 series were only partially successful because the thickness of the whole laminar coat was barely greater than the recoil distance. It is suggested that one or two interruptions at a distance slightly greater than 25μ from the kernel surface will be the most effective in limiting the growth of spearhead attack.

Laminar coatings are susceptible to peeling (lamination) both through external corrosive effects and internal shrinkage. ORNL [24] have shown

that steam at temperatures in the range 800-1100°C produces either severe lamination in the outer layers of laminar coatings or, if the coating is more of the featureless type, a more uniform type of corrosion. It is suspected that the external corrosion seen in some experiments results from steam produced from water vapour remaining either within the graphite components in the capsules due to incomplete degassing, or within the pores in the compacts which were not degassed at all prior to irradiation. Stringent pre-irradiation degassing procedures are in future to be applied to all the charges. From the irradiation tests so far examined it is not possible to say whether columnar coatings will laminate in the same way. Corrosion effects were not very pronounced in the HPD5 series, and since no columnar coatings have been applied directly to the kernel it is not known whether internal shrinkage would produce laminations in these coatings.

The ability of pyrocarbon to deform under certain irradiation conditions to cumulative strains of about 20% without cracking has been described. It is considered that this probably occurs under slow rates of strain, but whether fast neutron irradiation influences the behaviour is not known. The brittle radial cracks observed in HPD5/5B and 6A are probably the result of sudden loading, thermal shock, or sudden release of elastic stresses by corrosion effects.

Although pyrocarbon has been shown to deform elastically, the strains observed are too high to have occurred by purely elastic behaviour. The effect of sectioning a spherical shell of pyrocarbon subjected to both elastic and plastic strains will obviously affect the shape of the layers and, therefore, caution must be applied in the interpretation of the observed effects. This is a case where microradiography coupled with microscopy should be valuable.

5.6 Fission Fragment and Fast Neutron Damage to Pyrocarbon and Silicon Carbide

Two observations have been described which have been attributed to fission fragment damage:-

- (1) Shrinkage of the pyrocarbon layer adjacent to the fuel kernel. This is normally but not exclusively associated with spearhead attack.
- (2) High response of a zone around the fuel kernel or ahead of the diffusion zone to polarised light.

The only data on fission fragment damage to pyrocarbon and other possible coating materials (SiC, MgO, BeO, Al₂O₃) are from BMI [6]. Exposures have only been in the range 1 to 5×10^{14} fission fragments/cm² and at a temperature of 80°C (cf., doses up to 7×10^{17} fission fragments/cm² to temperatures up to 1700°C in the particle coatings) and hence the data are not necessarily very applicable. However, these experiments showed that all the materials expanded under bombardment from fission fragments, pyrocarbon and SiC showing the highest expansion. It was also found that firstly, most of the radiation induced expansion in the materials was removed on annealing at 1200°C, though the pyrocarbon samples did not give a clear result due to its anisotropic properties, and secondly, that an increase in dose from 10^{14} to 5×10^{14} fission fragments/cm² only gave a factor of 2-3 increase in expansion, suggesting a tendency towards saturation.

The observed effect in the irradiated particles is, however, an overall shrinkage of the fission fragment bombarded layer and hence the low temperature data cannot wholly apply. It is postulated, therefore, that the effect of the fission fragment bombardment is twofold:-

(i) The major effect is to cause a shrinkage; it is postulated that this results from an ordering or even graphitisation of the pyrocarbon into a denser form. Pyrocarbon as deposited on the fuel particles is turbostratic, that is, although the hexagonal layers are parallel to one another, and uniformly separated, they are orientated at random with respect to one another. The density of the deposit depends on the gas used, flow rate and temperature. For coatings prepared by pyrolysis of methane, the lowest density (1.4-1.6 g/cm²) occurs at deposition temperatures of ~1600°C. Unfortunately, the coatings are normally deposited at this temperature, for if they are applied at higher temperatures the uranium diffusion is too high and the coating becomes contaminated, and if applied at lower temperatures there was thought to be a risk that operation at temperatures higher than the coating temperature would cause cracking due to the higher thermal expansion of the fuel relative to the coating.

Pyrographite, however, has a density of 2.11-2.22 g/cm³. It has been found that thermal annealing in the presence of UO₂ of pyrocarbon deposited in a fluidised bed caused graphitisation at 2200°C [25], which was presumed to be due to the diffusion of uranium through the pyrocarbon. However, identical material not mixed with UO₂ could not be graphitised by heat treatment up to 2800°C. It is possible that the effect of fission fragment bombardment is to markedly reduce the temperature at which this transformation occurs. The characteristic V-shaped void is attributed to the larger degree of shrinkage in the more heavily damaged material adjacent to the kernel. This postulate, however, requires proof and the effects of fission fragment dose, temperature and density of coating on the process must be studied.

(ii) The secondary effect could be an expansion caused by the formation of vacancy-interstitial pairs. At 80°C the BMI workers [6] calculated that the observed expansion corresponded to about 10³ displacement atoms per fission fragment, but as would be expected, a large proportion of the damage was annealed out above 800°C. A further contribution in the high burn-up samples will be the accommodation within the lattice of the fission products either in an elemental state or combined with carbon.

There is little indication of a large variation in the amount of shrinkage caused by the fission fragment recoil atoms in pyrocarbon within the range of temperature and dose studied. This appears to indicate that saturation occurs below the lowest dose so far investigated, and further experiments are planned. Variation in coating density should, if the postulate is correct, have quite a marked effect and this will also be investigated.

In all the particles examined the initial coating has been either of the laminar or interrupted laminar type. It was, however, observed in the HPD5 series that a columnar second coating deposited at 1600°C did not halt the advance of spearheads as effectively as either of the laminar coatings or the columnar coating deposited at 1800°C. This would suggest that this type of coating is particularly affected by fission fragment bombardment; one possible mechanism for the advance of spearhead attack would be due to the fission fragments ejected further into the pyrocarbon from the fuel deposited on the inside surface of the spearhead by a process of knock-out from the kernel surface thus repeating the initial process. The existence of the layer has been shown by microprobe analysis, though what is not known at present is the chemical effect of fission products on the process. This will require active microprobe analysis to determine if there is an associated concentration of any fission products, e.g., formation and decomposition of caesium graphite during temperature cycling. Similarly mass transfer of carbon through a gaseous phase might also be occurring.

In the HPD4 and Studsvik tests triplex coatings were applied to the kernels. The initial pyrocarbon layer, however, was not sufficient in some batches to protect the silicon carbide from direct recoil bombardment. Measurements on SiC deposited at 1600°C show it is very dense (~ 95% theoretical density), and hence based on the pyrocarbon hypothesis one would expect little or no spearhead attack in SiC. This is borne out by observation. Most cracks in the SiC are parallel sided radial cracks apparently resulting from the release of internal or thermal stresses. It appears, therefore, that SiC, though more prone to thermal stress cracking, may well be more resistant to spearhead attack than pyrocarbon. This conclusion requires further tests under strictly comparable conditions of temperature and burn-up.

The data on fast neutron damage at 600°C to pyrolytic graphite (high density pyrocarbon deposited at 2200°C) would indicate that a pyrolytic coating should decrease in circumference ('a' direction) and have a slight increase in thickness ('c' direction). No directly relevant data on pyrocarbon at high temperatures are available. In the particles examined it was impossible to determine whether any dimensional changes had occurred in the outer layers of the coating: in any case the fission fragment effects in the inner layer appear to be so much larger, and result in a shrinkage away from the outer layer, that small changes in dimension of the outer coating are relatively unimportant.

The total fast neutron dose to which these coatings have been subjected is partly self-generated from fission of the kernel, the remainder being from the reactor flux. No obvious differences which could be attributed to fast neutron damage were observed between the HPD series and the remaining experiments, although the HPD series were irradiated in an in-core position and had a fast neutron flux approximately two orders of magnitude higher than the DY and Pluto Loop irradiations. In pyrocarbon coatings irradiated as in this programme fast neutron damage does not, therefore, appear to be a major factor in determining the integrity of a particle.

Fast neutron irradiation of SiC has shown that isotropic expansion of the order of 1% occurs after an integrated fast neutron dose of $4.6 \times 10^{20} \text{ n/cm}^2$ at 150°C [26]. As yet, no higher temperature data is known, but it would be expected that the changes would be far smaller at the temperatures of interest in an HTR. It seems likely that this will not be a major problem,

though full term burn-up tests on the triplex type of coating are necessary to ensure that differential changes between SiC and pyrocarbon will not cause excessive stresses.

SUMMARY AND CONCLUSIONS

- (1) The function of a coating around a fuel kernel is to contain as much of the fission product activity as possible. Fission gas release from lightly irradiated particles is normally very low and arises from three sources: fuel contamination in the outer few microns of the coating, diffusion of fission products through the coating, and particles with cracked coatings. A substantial increase in release rate during irradiation is deemed to constitute failure and will occur if the coating is fractured, or if the fuel has migrated to within fission fragment recoil distance ($\sim 20\mu$) of the outer surface either by diffusion or by 'spearhead' attack.
- (2) Most of the fuel kernels tested in this programme were sintered and of fairly high porosity in contrast to the U.S. approach which was to use high density melted kernels. Apart from possible cost advantage, sintered particles provide a means whereby sufficient voidage can be provided to accommodate both the fuel swelling due to solid fission products and the pressure exerted by the release of the gaseous fission products, which in the most pessimistic case was assumed to be 100%. No serious disadvantages to the approach have been revealed and the marked densification that occurred in the UC_2 kernels at irradiation temperatures as low as $800^\circ C$ appeared to give the advantages of both approaches. Very low failure rates have been obtained at burn-ups of up to 8% fima and irradiation temperatures up to $1300^\circ C$ using sintered UC_2 kernels coated with a double laminar pyrocarbon coat.
- (3) A qualitative correlation between fission gas release and the number of failed particles observed has been obtained in all except the Pluto Loop IIIA test. This appears to show that, even in particles with failed coatings, the UC_2 retained $\sim 99\%$ of its fission product gases and at the same time was remarkably swelling resistant. This behaviour is contrary to U.S. experience, and the differences have not been resolved. It was also shown that out of pile annealing 'transients' to $1800^\circ C$, i.e., $600^\circ C$ above the normal in-pile operational temperature, caused neither cracking of intact particles nor further release of fission gas.
- (4) In addition to undiluted UC_2 , $(Zr,U)C$, specifically designed for the Dragon reactor, and $(Th,U)C_2$ fuels have been tested in both melted and sintered forms. Neither the sintered $(Zr,U)C$ nor $(Th,U)C_2$ kernels appear to densify as markedly as UC_2 under irradiation, even at temperatures of $1700^\circ C$. $(Zr,U)C$ kernels can apparently withstand higher operational temperatures than UC_2 without marked diffusion of the fuel into the coating occurring. Melted, polycrystalline $(Zr,U)C$ kernels appear essentially unchanged by irradiation. The melted $(Th,U)C_2$ kernels, which were monocrystals, either cracked which resulted in cracks also occurring in the coating, or appeared to undergo a phase transformation. Neither of the alloyed kernels have yet been tested to such high burn-ups as UC_2 , and hence a complete comparison cannot be made.
- (5) The outstanding advantage of SiC over pyrocarbon as a coating material is its superior retention of barium, strontium and caesium. It has been

tested as the "meat" in a triplex pyrocarbon/silicon carbide/pyrocarbon sandwich coating. These coatings have not yet been tested in conjunction with such high burn-up particles as pyrocarbon alone, but excellent results have been obtained so far using them in conjunction with both sintered and polycrystalline melted kernels. Radiochemical analyses for the solid fission product release in these tests are not yet complete. In particles where the inner pyrocarbon layer was very thin, direct fission recoil did not appear to damage the silicon carbide.

(6) Spearhead attack, the formation of characteristic V-shaped cracks extending radially outwards into the first 20-25 μ of the pyrocarbon coating, is observed in nearly all particles. This fission fragment bombarded layer was optically active under polarised light in contrast to the adjacent undamaged coating. It is tentatively postulated that spearhead attack results from the shrinkage of the low density pyrocarbon, the fission fragment bombardment causing ordering or perhaps graphitisation of the pyrocarbon. Failure of a coating normally occurs through the outward growth of spearhead attack or cracks associated with it. The cause of this growth is not clear and there may be more than one phenomenon operating. Effects apparently resulting from both internal pressure and internal corrosion which might be either gaseous or associated with fission products have been observed. External corrosion, probably from water vapour, has also been responsible for some failures.

(7) Spearhead attack has often been observed to have been halted by definite interruptions between two laminar pyrocarbon coatings. A test incorporating a pseudo-interrupted inner laminar coat with either a laminar or columnar outer coating emphasised that these interruptions can be effective though there are some, as yet, unexplained failures. A combination of this modified laminar inner coat with a columnar type outer coat deposited at 1800°C gave consistently good results.

7. ACKNOWLEDGMENTS

The authors are very conscious of the fact that a very large number of people have taken part in the many stages involved in an irradiation programme of this magnitude, and this report is the culmination of a great deal of work. All the work, with the exception of the early AERE fabrication and irradiation tests, has been performed within the Dragon Project either directly or under contract. As it would be invidious to mention specific names the major groups that have taken part are listed only:-

Fuel Element Fabrication Group,	Met. Div. AERE	Kernel fabrication.
Irradiation Services Group,	" " "	Rigs and post-irradiation services.
High Activity Handling Group,	Eng. Div. "	Post-irradiation handling.
Graphite Technology Group,	Chem. Eng. Div. AERE	Coating.
Fission Product Technology Group,	Chem. Div. AERE	Fission product analysis.
Pluto Loop Users Group,	Chem. Div. "	Pluto Loop operation.
Fuel Element Development Group,	Dragon Project	Particle preparation.
Dragon Irradiation Facilities Group,		Irradiation preparation.

Active Handling Group,	A.B. Atomenergi, Studsvik	Post-irradiation handling.
Radio-chemistry Group,	" " "	Fission Product analysis.
Danish AEK, Riso		Irradiations.
S.G.A.E. Seibersorf		Pre-irradiation assessments.

The authors regret that they are unable to reference the large number of Dragon Project Reports that have been used in the preparation of this report in order that it may be published in an unclassified form.

Finally, acknowledgment must be made to Mr. R. A. U. Huddle for the overall direction of the programme, and the help and encouragement given during the preparation of this report. The authors wish to thank Mr. C. A. Rennie, the Chief Executive of the Dragon Project, for permission to publish this paper.

REFERENCES

- [1] A. K. Smalley, et al, BMI - 1483 (1962).
- [2] "Ceramic Matrix Fuels Containing Coated Particles," BMI Symposium (1962) TID 7654.
- [3] A. W. Hare and F. A. Rough, BMI - 1491 (1962).
- [4] D. I. Sinizer, et al, IAEA Symposium (May, 1962).
- [5] H. H. Yoshikawa, TID - 7654 (Nov., 1962) p.273.
- [6] T. S. Elleman, et al, BMI - 1635 (1963)
- [7] R. Flowers, et al, AERE, Unpublished Work.
- [8] M. L. Bleiberg, WAPD - 263.
- [9] J. B. Sayers, Quoted by P. Murray, Nuc. Eng. February, 1962.
- [10] O. S. Plail, Nuc. Eng. January, 1961, p.82.
- [11] R. A. Saunders, Nuc. Eng. January, 1963, p.15-19.
- [12] F. Sterry, AERE, Unpublished Work.
- [13] P. E. Reagan, et al, TID - 7654 (Nov. 1962) p.94.
- [14] F. Rough and W. Chubb, BMI - 1448 and NAA - SR - 5350 (1960).
- [15] A. Accary, Private Communication (1963).
- [16] W. Goeddel, TID - 7654 (Nov. 1962) p.187.
- [17] W. O. Harms, IBID, p.88.
- [18] R. S. Sharpe, AERE - R4252 (1963).
- [19] P. E. Reagan, et al, ORNL - 3445 (March 1963) p.147.

- [20] L. R. Zumwalt, et al, TID - 7654 (Nov., 1962) pp.223-272.
- [21] R. M. Carroll, et al, ORNL - 3372 (Sept., 1962) p.235.
- [22] R. W. Dayton, et al, TID - 7654 (Nov., 1962) p.62.
- [23] R. J. Burian, et al, BMI - 1628 (1963).
- [24] L. Overholser, et al, ORNL - 3445 (March, 1963) p.180.
ORNL - 3372 (Sept., 1962) p.259.
- [25] A. Auriol, et al, AIEA Symposium (July, 1963).
- [26] R. Hawes (AERE), Private Communication (1963).
- [27] N. R. Williams, AERE - M 1116.
- [28] K. W. Carley-Macaulay, J. W. Myles and G. H. Williams, "Paper to Symposium on Carbides in Nuclear Energy," (AERE, Nov., 1963).
- [29] J. Henney, D. T. Livey and N. A. Hill, AERE - R4175 and 4176.

Table 4

Details of Pyrocarbon Coated UC_2 Particles for P1, DY and HPD2 Charges

Charge	Pluto P1	Dido DY and HPD2				
Kernel Fabrication	Prepared from UO_2 using Williams [27] process UC_2 spheroids reacted at 1400°C, followed by further sintering at 1600°C, Density ~70% theoretical	Prepared from UO_2 using Williams [27] process UC_2 spheroids reacted at 1500°C, Density ~70% theoretical				
Coating Details [28]						
Batch No.	HT 46	HT 69	HT 70			
Av. Kernel dia. (μ)	290	190	188			
Coating Conditions						
Stage 1 Pre-coat Temp. °C	1500-1830	1450-1650	1450-1650			
Main coat temp. °C	1830	1650	1650			
Coating thickness (μ)	42	25	28			
Stage 2 Main coat Temp. °C	1850	1650	1650			
Coating thickness (μ)	25	37	36			
Av. Total coating thickness (μ)	69	62	64			
Type of pyrocarbon	Laminar	Laminar	Laminar			
Pre-Irrad. Testing						
Fraction core leached	8.3×10^{-6}	N.D.	N.D.			
α-assy. U visible U in core	3.7×10^{-5}	1.8×10^{-5}	2.7×10^{-5}			
Light Irrad. Data						
Cumulative fractional release of Xe-133 on annealing at 1500°C	6 h 4.4×10^{-6} 24 h 7.3×10^{-6} 48 h 1.1×10^{-5} 72 h 1.4×10^{-5}	24 h 3.8×10^{-5} 48 h 4.8×10^{-5} 72 h 6.3×10^{-5} 100 h 8.5×10^{-3}	6 h 2.7×10^{-6} 24 h 7.5×10^{-6} 48 h 9×10^{-6} 72 h 9×10^{-6} 100 h 9×10^{-6}			
Irradiation Capsule Identification	P1	DY 3-10	DY 1 and 2 HPD2 Compacts 1-6			
Irradiation Conditions						
Average Irradiation			Capsules		Capsules	
Temp. °C	800	3,4	5,6	7,8	9,10	DY 1,2
Burn-up % Fima	9	1300	925	1275	1000	1250
% Fifa	9	7.3	6.6	4.3	3.3	7.1
No. of days full power	144	7.3	6.6	4.3	3.3	7.1
No. of major thermal cycles	47			43		43
				6		20
					6	20

Table 5
Details of Particles in HPD4 Charge

HPD4	Pre-Irradiation and Irradiation Data	$(\text{Th}, \text{U})\text{C}_2$	$\text{Th}/\text{U-235} = 5$	$(\text{Zr}, \text{U})\text{C} \frac{\text{Zr}}{\text{U-235}} = 5$
Kernel Fabrication	<p>Starting materials Enrichment of Uranium (U-235) Excess Carbon</p> <p><u>Sintering</u> conditions - Temp. - Time - Atmos.</p> <p>Melting in plasma arc Density (g/cm^3) - Theoretical - Xylene - Mercury</p> <p>X-ray analysis</p>	$\text{UC}_2 + \text{Th} + \text{C}$ 23.02 0.24 2000°C 4 h Vacuum No 9.89 9.3 5 ThC_2 lines	$\text{Th}/\text{U-235} = 5$ Yes 9.89 9.5 8 ThC_2 lines	$\text{ZrC} + \text{U} + \text{C}$ 92.73 stoichiometric 1800°C 1 h Argon Yes 8.05 7.6 7.3 ZrC lines (solid Solution)
Coating Details	<p>Kernel diameter (μ) Batch number</p> <p><u>1st Stage</u> Temperature (°C) Thickness (μ) Type</p> <p><u>2nd Stage</u> Temperature (°C) Thickness (μ) Type</p> <p><u>3rd Stage</u> Temperature (°C) Thickness (μ) Type</p> <p>Total Thickness (μ)</p>	+251 -353 C90 1460 8 1700 60 Sic (β) 1700 40 pyrocarbon, 108	+251 -460 C100 1350-1560 8 1600 41 Sic (β) 1700 32 pyrocarbon, 81	+251 -353 C142 1340-1600 22 laminar 1640 22 Sic (β) 1720 30 laminar 74
Pre-Irradiation Testing	<p>Fraction of core leached Fraction of core visible (1) (α-assay)</p> <p>Density of Coated particles (g/cm^3) Uranium Content of Coated Particles (wt. %)</p>	1.72×10^{-5} 0.06×10^{-5} 3.10 6.5	6.44×10^{-5} 0.06×10^{-5} 3.42 10.6	not leached 0.5×10^{-5} 4.02 20.3
Compacts	Compact fabricated from a mixture of graphite powder and binder; impregnated with PyC deposited from Benzene 12 h at 830°C	3 compacts	6 compacts of this batch, evenly distributed through the rig (one in each box)	3 compacts, distributed in Boxes 1, 3, 5
Irradiation Conditions	<p>Temperature (°C) Burn-up % fima % fifa</p> <p>No. of days full power No. of major thermal cycles</p>	RAUG 46 1030-1400 2.0-2.6 12-17 42 2	COMPACTS 1B (M Zr, 1325°C) 2A (M Th, 1350°C) 3A (M Th, 1400°C) 3B (M Zr, 1400°C) 4B (S Th, 1375°C) 6A (S Th, 1225°C)	EXAMINED annealed annealed annealed annealed

Table 6

Details of Pyrocarbon Coated (Zr, U)C Particles Irradiated in HPD5

Kernel Fabrication		Prepared from hafnium free ZrC and UC powders 5 vol. % excess carbon added. Spheres sintered at 2000°C for 4 h in vacuo. Density (in xylene) 7.06 g/cm ³ Av. closed porosity 4.8% (in Hg) 5.24 g/cm ³ Av. total porosity 35.0%			
Coating Details					
Kernel diameter (μ)		251-295			
1st stage Coating temp. °C		1600			
Total thickness (μ)		20-25			
Type of coating		This first stage actually consists of five steps, the partial pressure of methane being dropped after 25, 20, 10, 20 and 10 minute intervals to produce interrupted laminar coating			
2nd stage					
Batch No.		C200	C201	C202	C203
Coating temp. °C		1300	1600	1600	1450
Thickness (μ)		53	50	40	95
Coating structure		Columnar	Columnar	Laminar	Laminar
Total coating thickness (μ)		75	72	62	117
Pre-Irradiation Testing					
Fraction of core leached		-	-	6.7 x 10 ⁻⁴	8.0 x 10 ⁻⁵
a-assy. U visible U in core		-	-	-	-
Light irradiation data		-	-	-	-
Cumulative fractional release of Xe-133		20 h 4.2 x 10 ⁻⁵	5.5 x 10 ⁻⁷	5.5 x 10 ⁻⁷	$\left. \begin{array}{l} \\ \\ \end{array} \right\} <5 \times 10^{-7}$
		40 h 5.1 x 10 ⁻⁵	6.3 x 10 ⁻⁷	7.7 x 10 ⁻⁷	
		60 h 5.9 x 10 ⁻⁵	6.4 x 10 ⁻⁷	9.4 x 10 ⁻⁷	
		100 h 7.0 x 10 ⁻⁵	7.9 x 10 ⁻⁷	1.2 x 10 ⁻⁶	
		200 h 8.6 x 10 ⁻⁵		1.5 x 10 ⁻⁶	
Fractional release at end of test of other fission products - test time h		220	144	150	240
Ba-140		4.1 x 10 ⁻²	4.3 x 10 ⁻²	2.9 x 10 ⁻²	1.1 x 10 ⁻³
I-131		9.3 x 10 ⁻³	3.1 x 10 ⁻³	6.3 x 10 ⁻³	6.5 x 10 ⁻⁴
Cs-137		5.9 x 10 ⁻³	5.9 x 10 ⁻³	1.6 x 10 ⁻³	5.4 x 10 ⁻⁴
Compact Details		Charge contained 3 capsules of each type			
Irradiation Conditions					
Average irradiation temp. °C		Range covered 1350-1750°C			
Burn-up % Fima		2.0-2.7			
% Fifa		12-16			
No. of days at full power		40			
No. of major thermal cycles					

Table 5
Details of Particles in HPD4 Charge

HPD4	Pre-Irradiation and Irradiation Data	$(\text{Th}, \text{U})\text{O}_2$	$\text{Th}/\text{U-235} = 5$	$(\text{Zr}, \text{U})\text{C} \frac{\text{Zr}}{\text{U-235}} = 5$																																																		
Kernel Fabrication	<p>Starting materials Enrichment of Uranium (U-235) Excess Carbon</p> <p><u>Sintering conditions</u> - Temp. - Time - Atmos.</p> <p>Melting in plasma arc Density (g/cm^3) - Theoretical - Xylene - Mercury</p> <p>X-ray analysis</p>	$\text{UC}_2 + \text{Th} + \text{C}$ 23.00 0.24 2000°C 4 h Vacuum	$\text{ZrC} + \text{U} + \text{C}$ 92.73 stoichiometric 1800°C 1 h Argon	$\text{ZrC} + \text{U} + \text{C}$ 92.73 stoichiometric 1800°C 1 h Argon																																																		
Coating Details	<p>Kernel diameter (μ) Batch number</p> <table> <tr> <td><u>1st Stage</u></td> <td>Temperature (°C)</td> <td>+251 -353</td> <td>+251 -460</td> <td>+251 -353</td> </tr> <tr> <td></td> <td>Thickness (μ)</td> <td>C90</td> <td>C100</td> <td>C142</td> </tr> <tr> <td></td> <td>Type</td> <td>1460</td> <td>1350-1560</td> <td>1340-1600</td> </tr> <tr> <td><u>2nd Stage</u></td> <td>Temperature (°C)</td> <td>1700</td> <td>1600</td> <td>1640</td> </tr> <tr> <td></td> <td>Thickness (μ)</td> <td>60</td> <td>41</td> <td>22</td> </tr> <tr> <td></td> <td>Type</td> <td>SiC (β)</td> <td>SiC (β)</td> <td>SiC (β)</td> </tr> <tr> <td><u>3rd Stage</u></td> <td>Temperature (°C)</td> <td>1800</td> <td>1700</td> <td>1720</td> </tr> <tr> <td></td> <td>Thickness (μ)</td> <td>40</td> <td>32</td> <td>30</td> </tr> <tr> <td></td> <td>Type</td> <td>pyrocarbon,</td> <td>pyrocarbon,</td> <td>laminar</td> </tr> <tr> <td></td> <td>Total Thickness (μ)</td> <td>108</td> <td>81</td> <td>74</td> </tr> </table>	<u>1st Stage</u>	Temperature (°C)	+251 -353	+251 -460	+251 -353		Thickness (μ)	C90	C100	C142		Type	1460	1350-1560	1340-1600	<u>2nd Stage</u>	Temperature (°C)	1700	1600	1640		Thickness (μ)	60	41	22		Type	SiC (β)	SiC (β)	SiC (β)	<u>3rd Stage</u>	Temperature (°C)	1800	1700	1720		Thickness (μ)	40	32	30		Type	pyrocarbon,	pyrocarbon,	laminar		Total Thickness (μ)	108	81	74	ZrC lines ThC_2 lines	ThC_2 lines	ZrC lines (solid Solution)
<u>1st Stage</u>	Temperature (°C)	+251 -353	+251 -460	+251 -353																																																		
	Thickness (μ)	C90	C100	C142																																																		
	Type	1460	1350-1560	1340-1600																																																		
<u>2nd Stage</u>	Temperature (°C)	1700	1600	1640																																																		
	Thickness (μ)	60	41	22																																																		
	Type	SiC (β)	SiC (β)	SiC (β)																																																		
<u>3rd Stage</u>	Temperature (°C)	1800	1700	1720																																																		
	Thickness (μ)	40	32	30																																																		
	Type	pyrocarbon,	pyrocarbon,	laminar																																																		
	Total Thickness (μ)	108	81	74																																																		
Pre-Irradiation Testing	<p>Fraction of core leached Fraction of core visible (1) (α-assay)</p> <p>Density of Coated particles (g/cm^3) Uranium Content of Coated Particles (wt. %)</p>	1.72×10^{-5} 0.06×10^{-5}	6.44×10^{-5} 0.06×10^{-5}	not leached 0.5×10^{-5}																																																		
Compacts	Compact fabricated from a mixture of graphite powder and binder; impregnated with PyC deposited from Benzene 12 h at 820°C	3 compacts	6 compacts of this batch, evenly distributed through the rig (one in each box)	3 compacts, distributed in Boxes 1, 3, 5																																																		
Irradiation Conditions	<p>Temperature (°C) Burn-up % fima % fifa</p> <p>No. of days full power No. of major thermal cycles</p>	RAUGHES 1050-1400 2.0-2.6 12-16 42 2	COMPACTS 1B (M Zr, 1325°C) 2A (M Th, 1350°C) 3A (M Th, 1400°C) 3B (M Zr, 1400°C) 4B (S Th, 1375°C) 6A (S Th, 1225°C)	EXAMINED annealed annealed annealed annealed annealed																																																		

Table 6

Details of Pyrocarbon Coated (Zr,U)C Particles Irradiated in HPD5

Kernel Fabrication	<p>Prepared from bafnium free ZrC and UC powders 5 vol. % excess carbon added. Spheres sintered at 2000°C for 4 h in vacuo.</p> <p>Density (in xylene) 7.06 g/cm³ Av. closed porosity 4.8% (in Hg) 5.24 g/cm³ Av. total porosity 35.0%</p>			
Coating Details				
Kernel diameter (μ)	251-295			
1st stage Coating temp. °C	1600			
Total thickness (μ)	20-25			
Type of coating	<p>This first stage actually consists of five steps, the partial pressure of methane being dropped after 25, 20, 10, 20 and 10 minute intervals to produce interrupted laminar coating</p>			
2nd stage				
Batch No.	C200	C201	C202	C203
Coating temp. °C	1800	1600	1600	1450
Thickness (μ)	53	50	40	95
Coating structure	Columnar	Columnar	Laminar	Laminar
Total coating thickness (μ)	75	72	62	117
Pre-Irradiation Testing				
Fraction of core leached	-	-	6.7×10^{-4}	8.0×10^{-5}
α -assy. $\frac{\text{U visible}}{\text{U in core}}$	--	--	--	--
Light irradiation data				
Cumulative fractional release of Xe-133	20 h 4.2×10^{-5} 40 h 5.1×10^{-5} 60 h 5.9×10^{-5} 100 h 7.0×10^{-5} 200 h 8.6×10^{-5}	5.5×10^{-7} 6.3×10^{-7} 6.4×10^{-7} 7.9×10^{-7}	5.5×10^{-7} 7.7×10^{-7} 9.4×10^{-7} 1.2×10^{-6} 1.5×10^{-6}	5.5×10^{-7} 7.7×10^{-7} 9.4×10^{-7} 1.2×10^{-6} 1.5×10^{-6}
Fractional release at end of test of other fission products - test time h	220	144	150	240
Ba-140	4.1×10^{-2}	4.3×10^{-2}	2.9×10^{-2}	1.1×10^{-3}
I-131	9.3×10^{-3}	3.1×10^{-3}	6.3×10^{-3}	6.5×10^{-4}
Cs-137	5.9×10^{-3}	5.9×10^{-3}	1.6×10^{-3}	5.4×10^{-4}
Compact Details	<p>Charge contained 3 capsules of each type</p>			
Irradiation Conditions				
Average irradiation temp. °C	Range covered 1350-1750°C			
Burn-up % Fima	2.0-2.7			
% Fifa	12-16			
No. of days at full power	40			
No. of major thermal cycles				

Table 7
Details of Pyrocarbon Coated UC_2 Particles Irradiated in Pluto Loop Charge IIIA

Kernel Fabrication		Prepared from UO_2 using Williams process. Reacted at 1400°C for 3 h to produce spheroids of density 5.5 g/cc						
<u>Coating Details</u>		C20 178-250	C27 128-178	C28 128-178	C29 128-178	C30 178-250	C31 128-178	C32 128-178
Batch No.								
Kernel Diameter								
<u>Coating Conditions</u>								
<u>Stage 1</u>	Temp. $^{\circ}\text{C}$	1300	1300	1350	1350	1350	1350	1350
	Time m	10	20	20	20	20	20	20
<u>Stage 2</u>	Temp. $^{\circ}\text{C}$	1650	1600	1600	1600	1600	1600	1600
	Time m	90	60	60	60	30	60	60
<u>Stage 3</u>	Temp. $^{\circ}\text{C}$		1400	1400	1400	1400	1430	1430
	Time m		25	40	40	100	50	45
Average Coating Thickness (μ)		153	64	61.5	54.5	55	78	77.5
Weight of UC_2 particles in charge g		5.0	10.52	11.2	10.39	7.73	9.22	5.27
<u>Pre-Irradiation Testing</u>								
Fraction of core leached				7.5 $\times 10^{-3}$ - 9.4 $\times 10^{-3}$				
α -assy				0.2% of core visible				
Light Irradiation Data								
Cumulative fractional release of				20 h at 1000°C	0.31 $\times 10^{-4}$			
Xe-133 on annealing				40 h at 1500°C	2.2 $\times 10^{-4}$			
				60 h at 1500°C	2.7 $\times 10^{-4}$			
				80 h at 1500°C	3.4 $\times 10^{-4}$			
				92 h at 1500°C	3.6 $\times 10^{-4}$			
Compact Details	Compacted into matrix using mixture of fine graphite powder and binder. Impregnated with pyrocarbon for 18 h $350-390^{\circ}\text{C}$							
<u>Irradiation Conditions</u>		Range in Loop	Insert 2	Insert 5	Insert 9			
Average Irradiation Temp. $^{\circ}\text{C}$		700-1200	800	100	1150			
Burn-up % Fifa		7-14	8	12	14			
% Fifa		7-14	8	12	14			
No. of days at full power		83*						
No. of major thermal cycles		20*						

* 8 transients cycled in fast reactor cycle to produce temperatures in fuel 200°C higher than normal operating temperature.

Table 8
Details of Particles in Studsvik I Charge

Studsvik I Loops	Pre-Irradiation and Irradiation Data	$(\text{Th}, \text{U})\text{C}_2 \frac{\text{Th}}{\text{U-235}} = 0.55$ (nominal = 10)		
Kernel Fabrication	Starting materials	$(1) \text{U} + \rightarrow \text{UC}_2$ (sintering 3 h in vacuo 1500°C) $(2) \text{UC}_2 + \text{Th} + \text{C}$		
	Uranium enrichment (U-235%)	93.09		
	Sintering Conditions	Temperature 2000°C Time 4 h Atmosphere Vacuum (10^{-3} mm Hg)		
	Composition of Sintered Particles	$\text{U} = 8.87\% \text{ Th} = 81.52\%$ $\text{U} = 8.30\% \text{ Th} = 81.03\%$		
	Melting in plasma arc	No		
	Density (g/cm ³) = (Theoretical Xylene	2.76 8.0		
	"X-ray analysis"	ThC ₂ lines + faint ThO ₂ lines		
	Kernel diameter (μ) Batch Number	-353 +251 683		
	1st Stage	Temperature (°C) Thickness (μ) Type		
	2nd Stage	Temperature (°C) Thickness (μ) Type		
	3rd Stage	Temperature (°C) Thickness (μ) Type		
	Total Thickness (μ)	121		
Coating Details	Fraction of core visible (d-assy.)	3.2×10^{-6}		
	Density of coated particles	3.33		
	Uranium content of coated particles (Wt. %)	4.21		
	Crushing strength (g)	2100		
	Light Irradiation Data	Fractional release of Xe-133 at 1500°C - after 27 h - after 200 h		
		1.5×10^{-5} 2.1×10^{-4}		
Pre-Irradiation Testing	Same procedure as for HDM	Two compacts containing these particles were in Loop A		
		The four compacts containing melted particles were in Loops B and C		
Irradiation Conditions		Loop A	Loop B	Loop C
	Temperature (°C)	(Helium (Neon		
		900-1000 970-1150		
	Burn-up % fima % fifa	1.2 13.4 37		
	No. of days at full power	1.15 12.8 37		
	No. of major thermal cycles	7		
	Average thermal flux (n/s/cm ²)	0.78×10^{14}		
	Compacts examined microscopically	0.75×10^{14} B_1		
		1.07×10^{14} C_1		

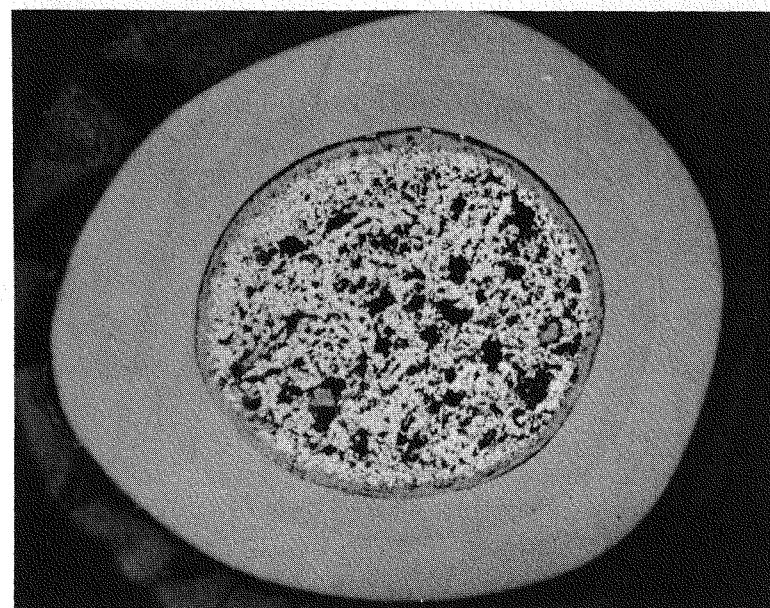


Fig. 1 DY; Unirradiated Particle (X250)



Fig. 2 PL IIIA/2; Typical Particle (X250)

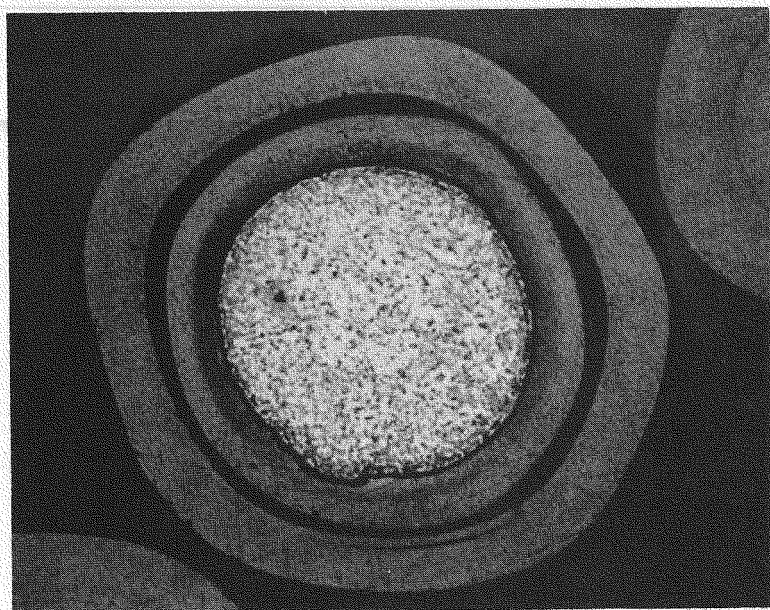


Fig. 3 DY7; Typical Particle (X250)

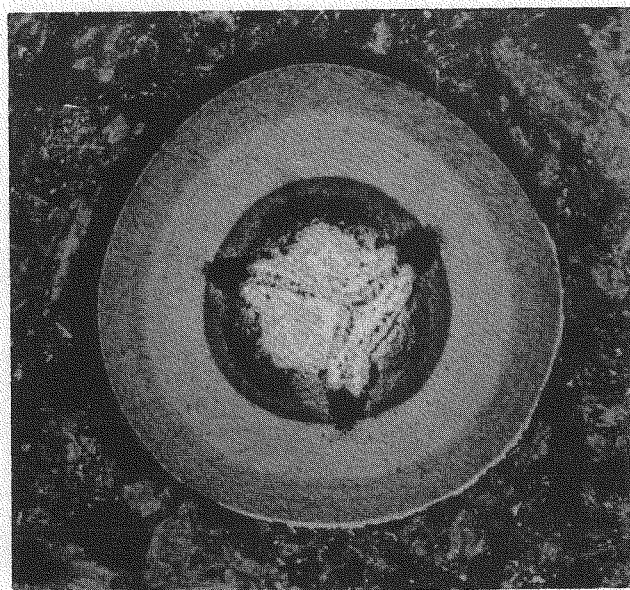


Fig. 4 PL IIIA/5; Typical Particle (X250)

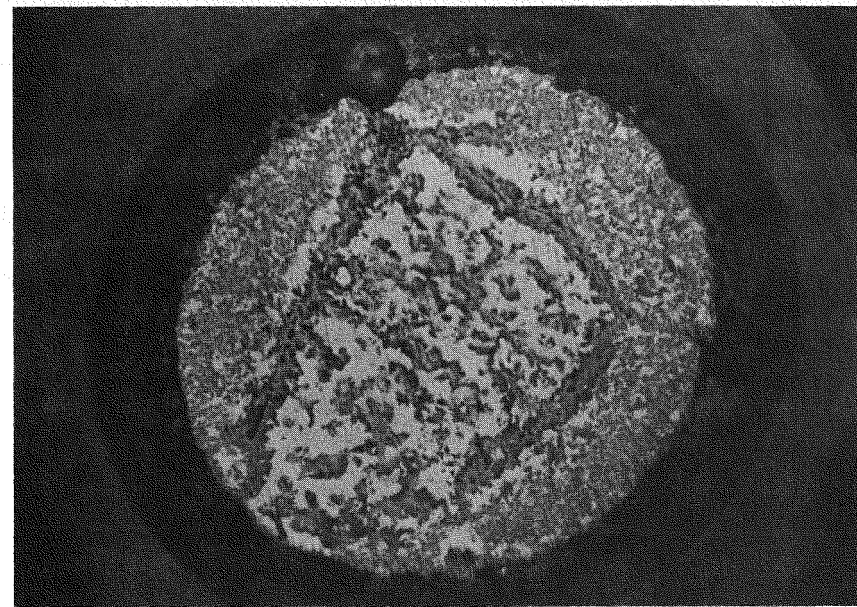


Fig. 5 PL IIIA/1; Details of Structure of Kernel
and Spearhead Attack

(X570)

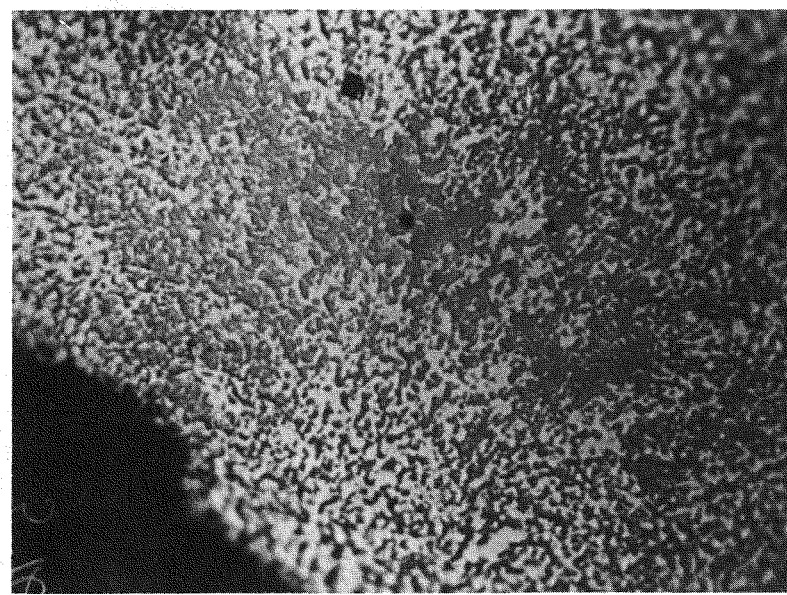


Fig. 6 PL IIIA/2; Structure of Kernel

(X1000)

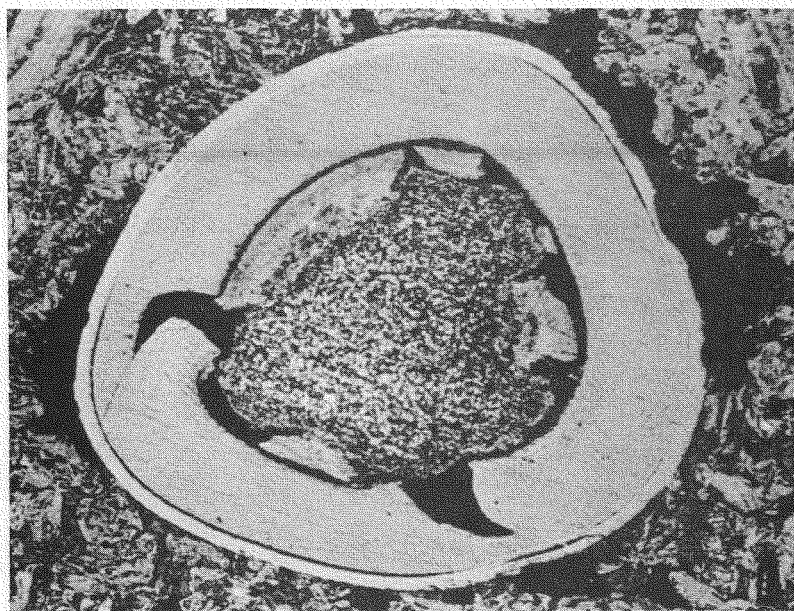


Fig. 7 PL IIIA/7; Large Spearheads Penetrating the Coating

(X250)



Fig. 8 DY5; Diffusion of Fuel into Coating; Kernel has a low density and has an inclusion of graphite at its centre

(X250)

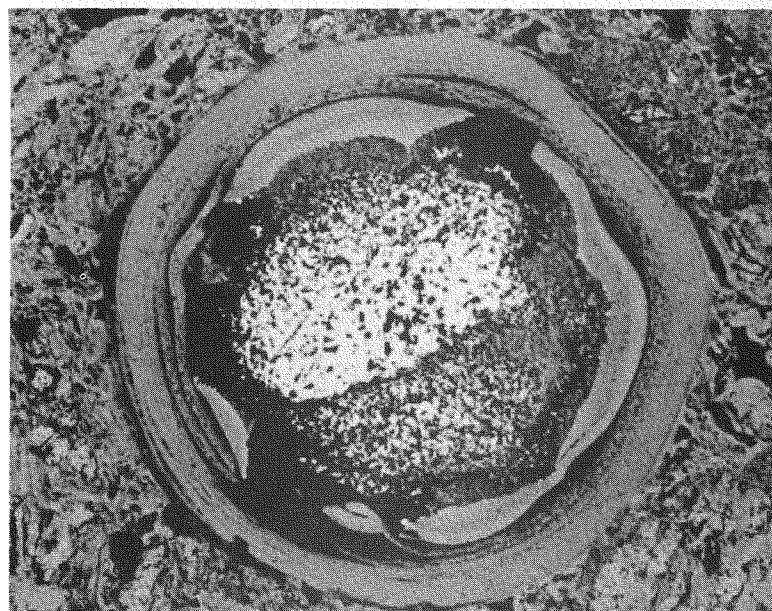


Fig. 9 HPD2/3; Diffusion of Fuel and Coating (X250)

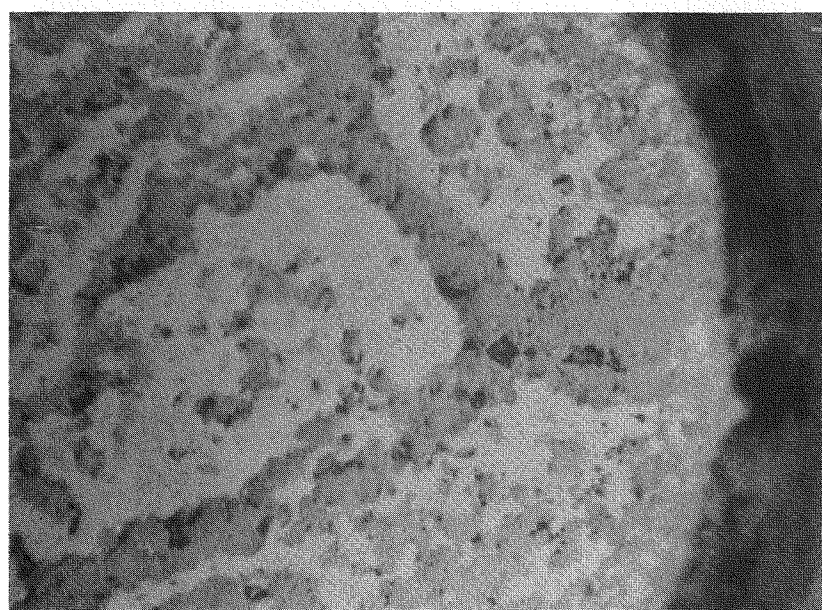


Fig. 10 PL IIIA/5; Details of Fine Precipitate in Carbide Phase (X250)

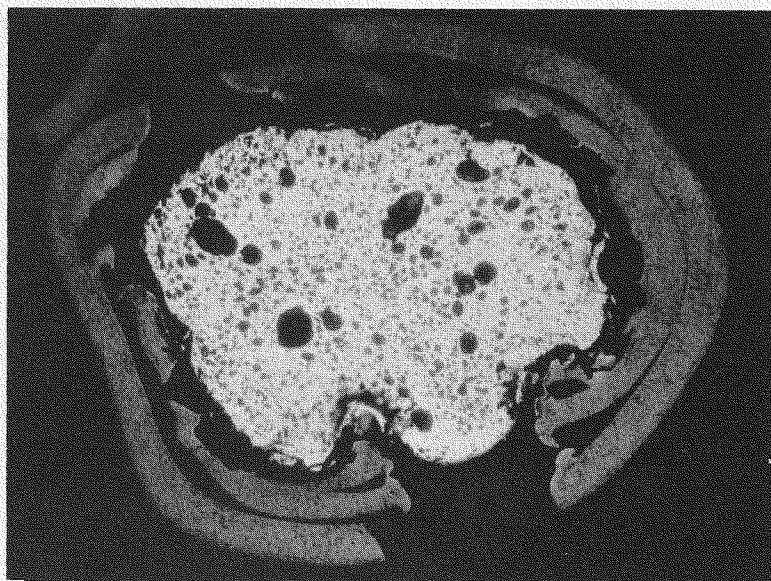


Fig. 11 P1; Broken Particle (X190)

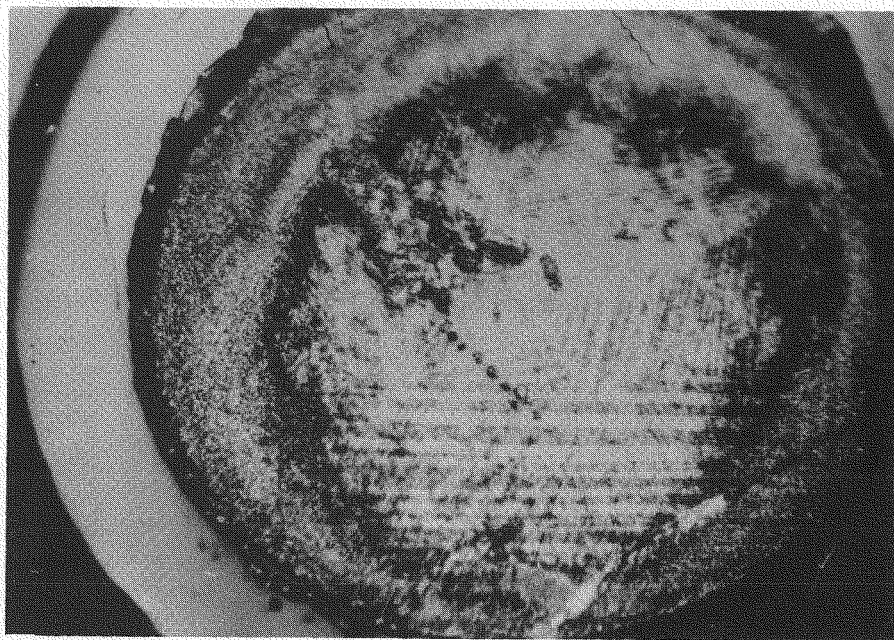


Fig. 12 HPD4/3A; Structure of Partially Recrystallised Kernel (X380)

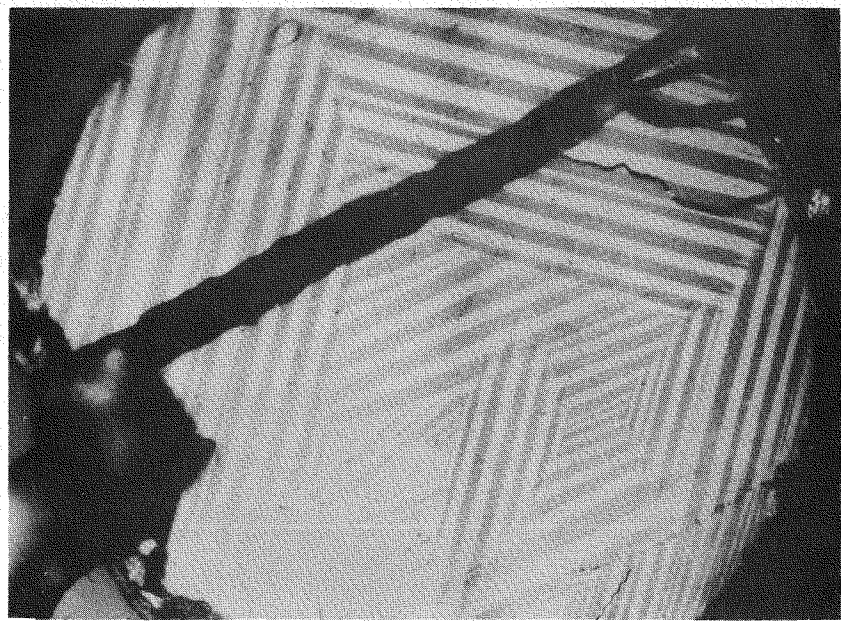


Fig. 13 HPD4/2A; Structure of Un-Recrystallised kernel (X350)

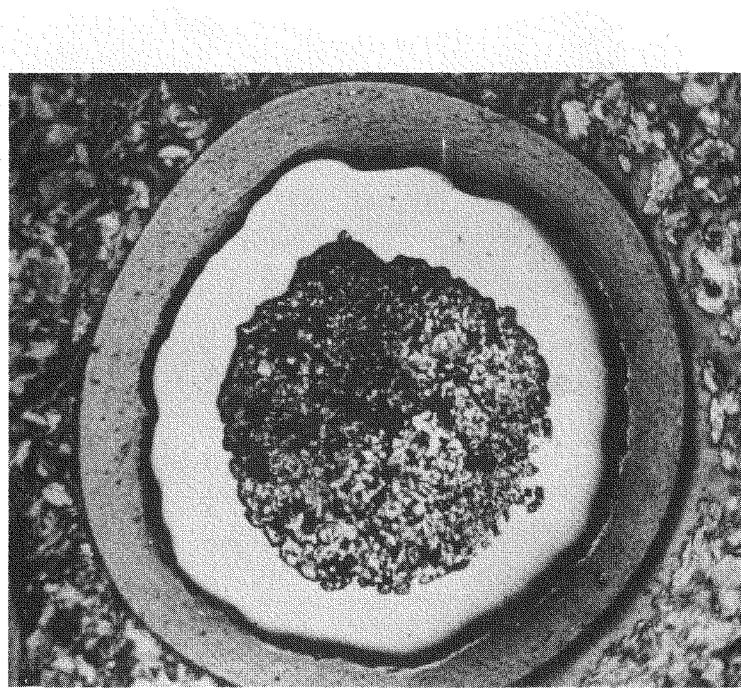


Fig. 14 HPD4/4B; Typical Particle (X150)

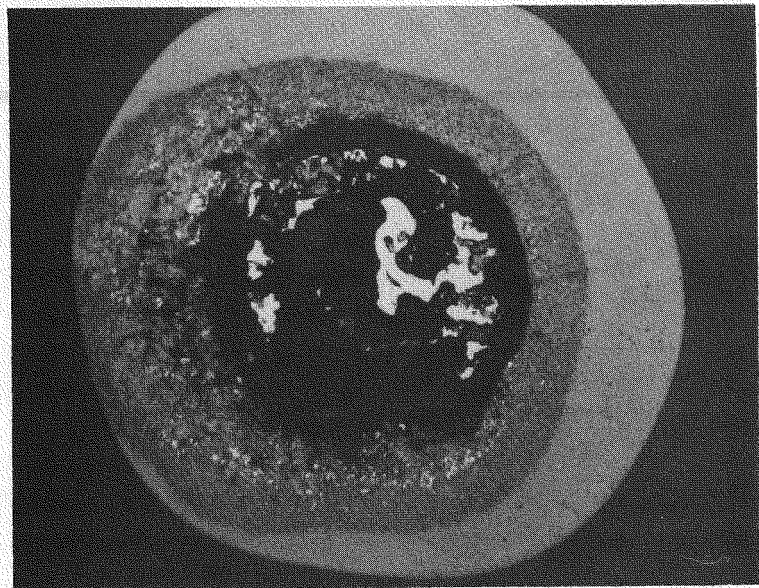


Fig. 15 DY; Unirradiated, showing Diffusion of Fuel through Coating at 2200°C

(X240)

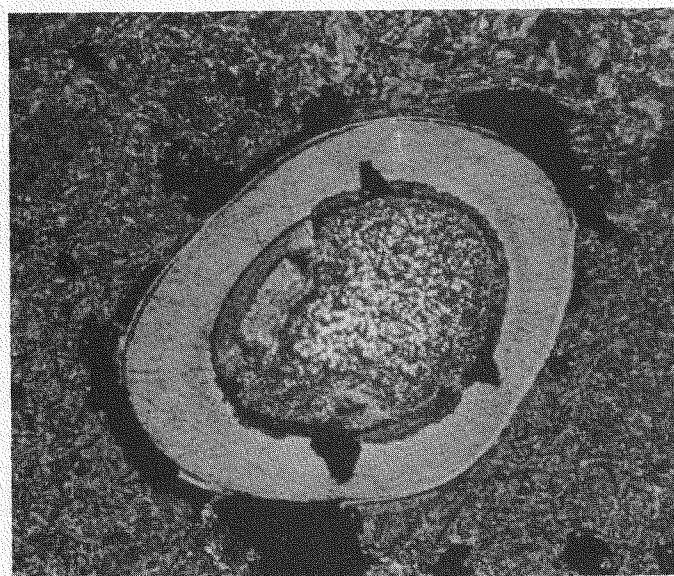


Fig. 16 PL IIIA/7; Diffusion Zone Extending 5 μ

(X250)

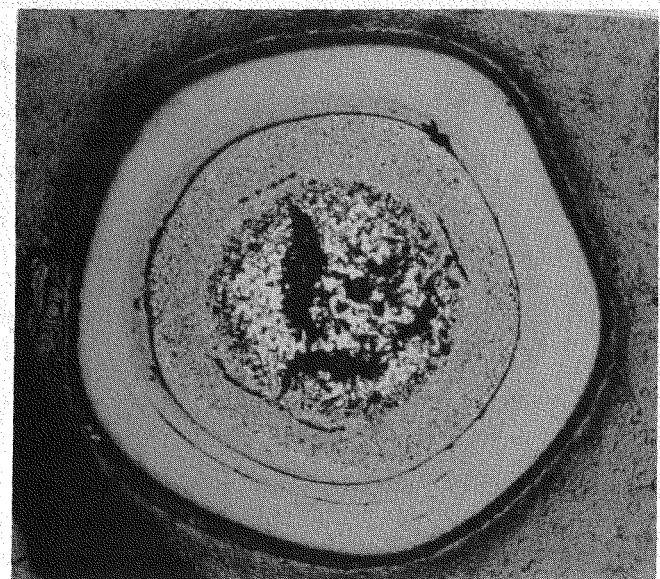


Fig. 17a DY1; Diffusion of Fuel into Coating

(X250)

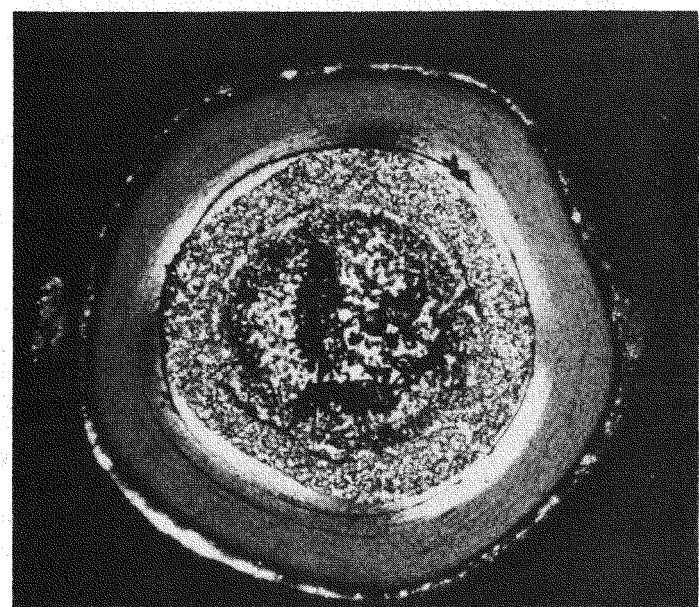


Fig. 17b DY1; As Fig. 17a under Polarised Light

(X250)

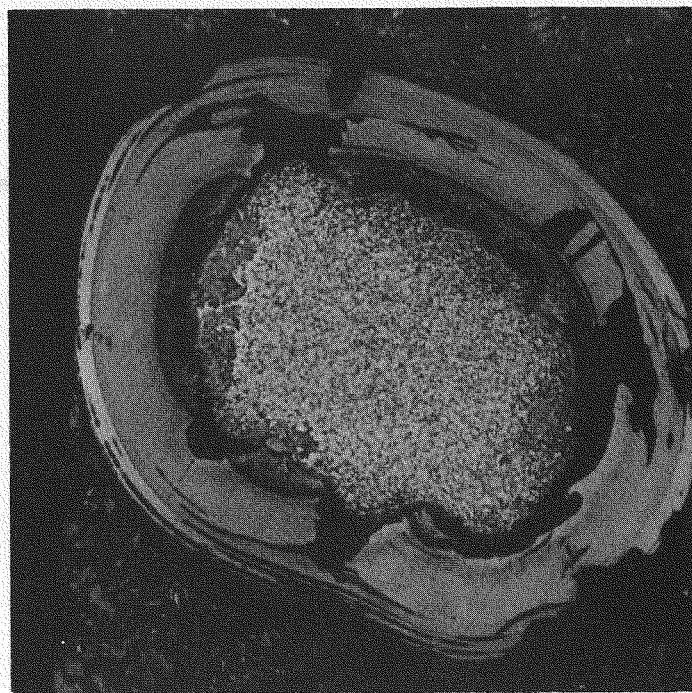


Fig. 18 PL IIIA/9; Severe Lamination of Coating caused by External Corrosion

(X250)

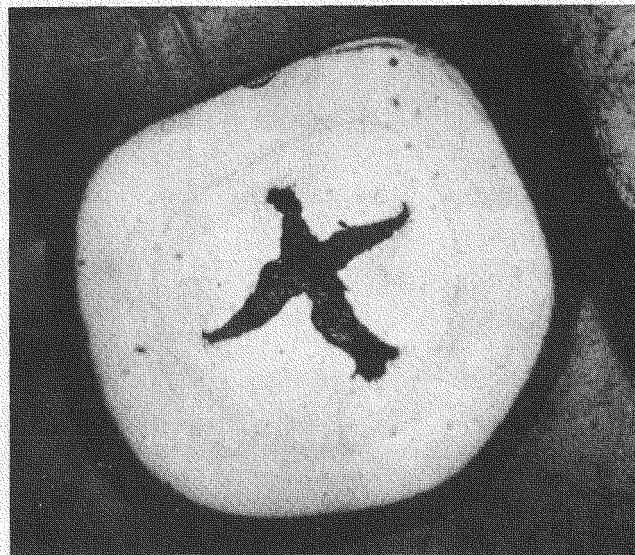


Fig. 19 Characteristic Shape of Spearhead Attack

(X275)

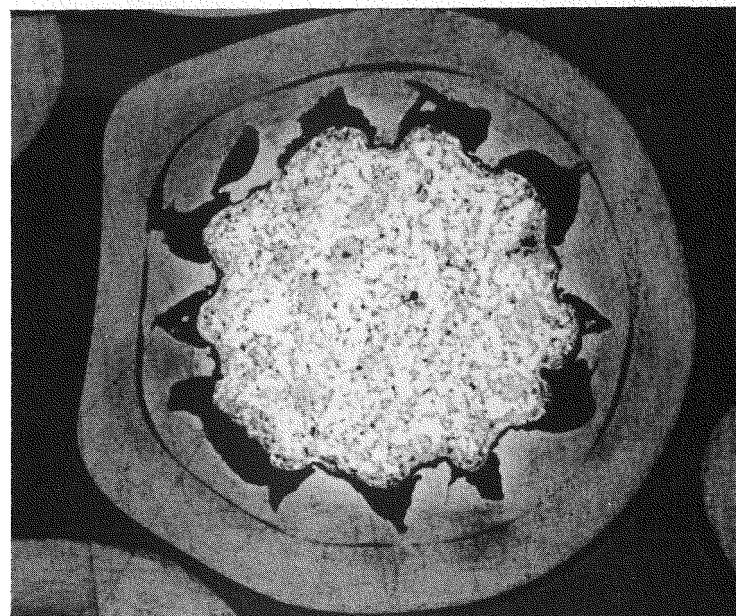


Fig. 20 DY7; Spearhead Attack and Swelling of Kernel into Voids (X250)

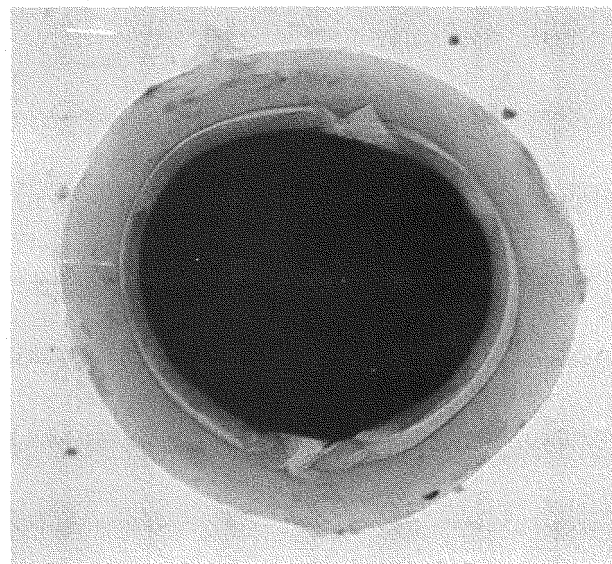


Fig. 21 P1; Microradiograph showing Spearhead Attack (X160)

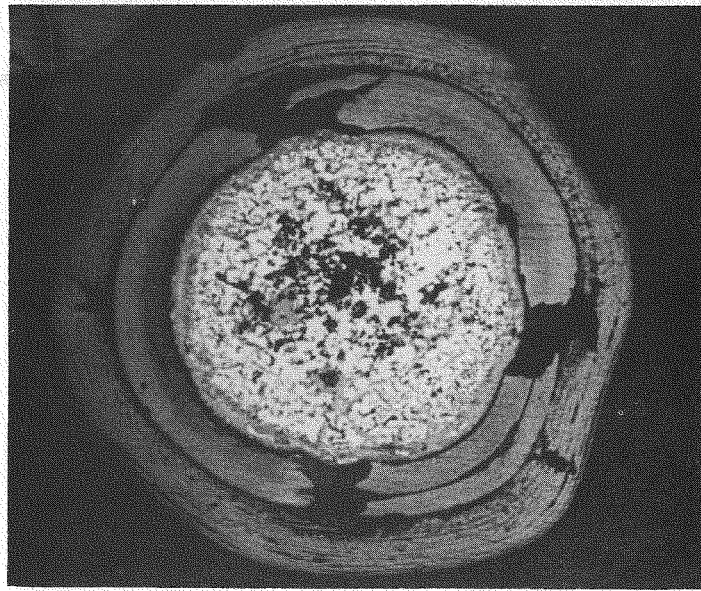


Fig. 22a DY1; Particle under White Light (x250)

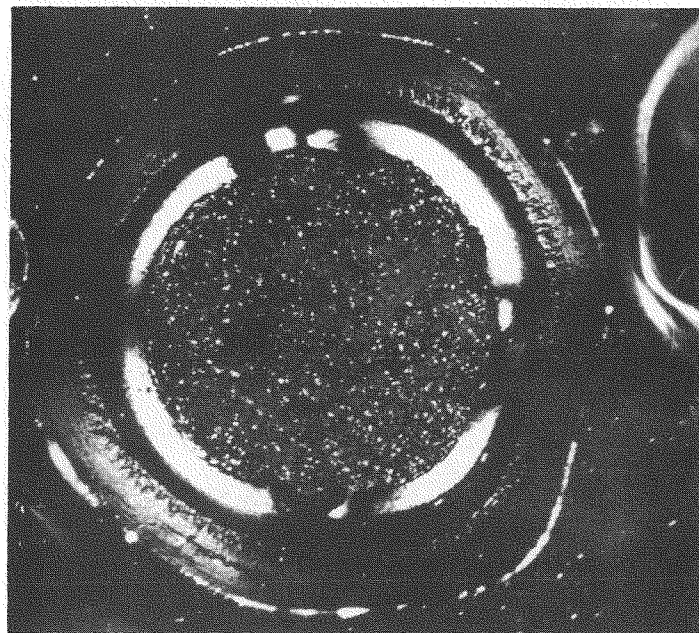


Fig. 22b DY1; As Fig. 22a under Polarised Light (x250)

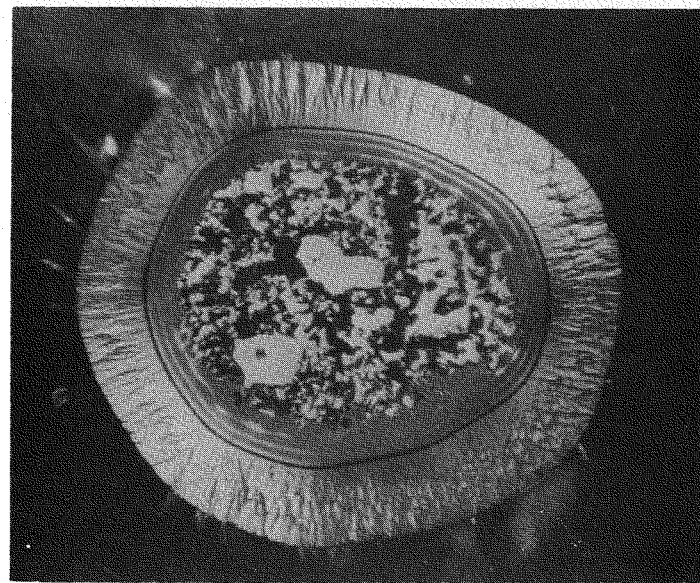


Fig. 23 HPD5; Coating Type C201, Unirradiated

(x160)

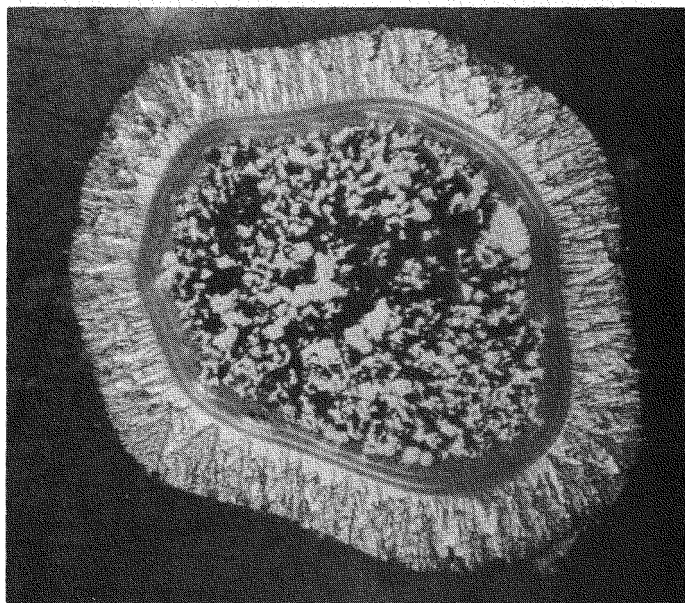


Fig. 24 HPD5; Coating Type C200, Unirradiated

(x160)

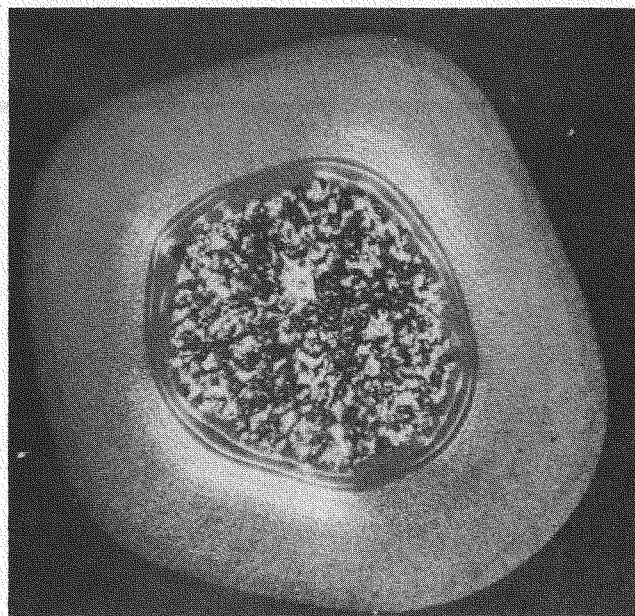


Fig. 25 HPD5; Coating Type C203, Unirradiated

(X160)

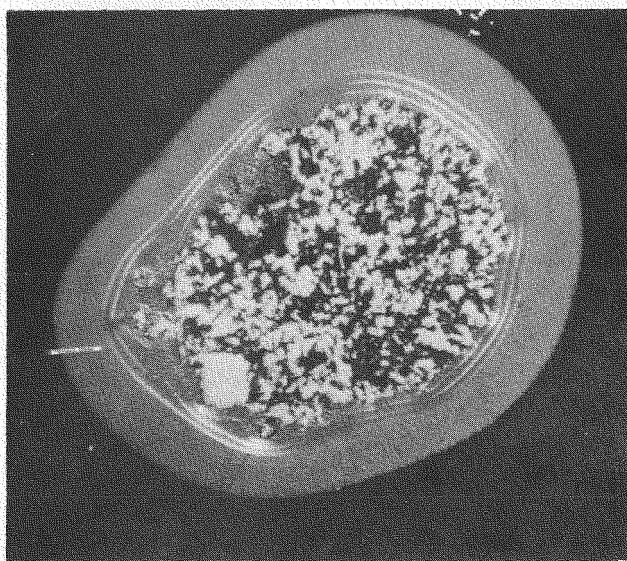


Fig. 26 HPD5; Coating Type C202, Unirradiated

(X160)



Fig. 27 HPD5/5A; Penetration of Spearhead Attack into Outer Columnar Coating (X154)

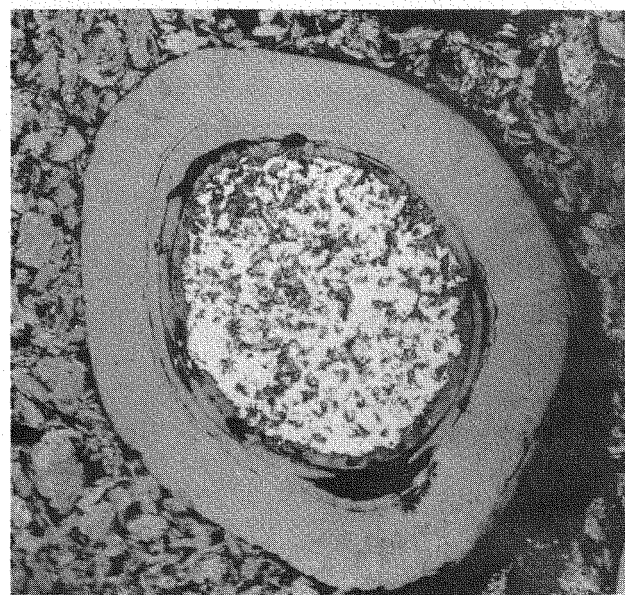


Fig. 28 HPD5/3A; Spearhead Attack Limited to Inner Coating (X154)

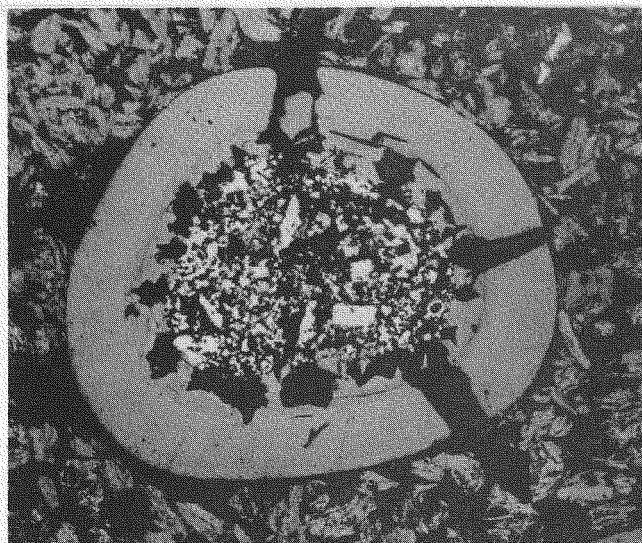


Fig. 29 HPD5/5B; Coatings Fractured by Wide Radial Cracks (X154)

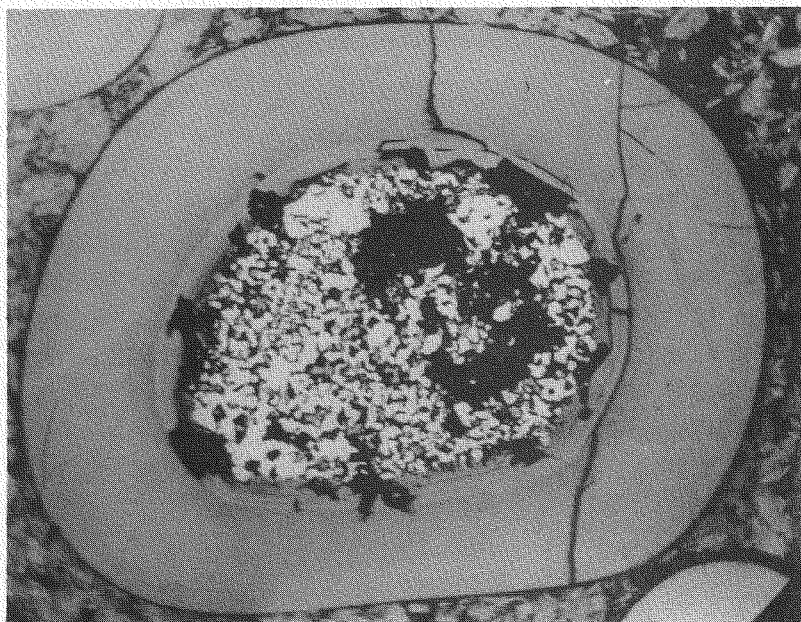


Fig. 30 HPD5/6A; Hairline Cracks in Coating (X154)

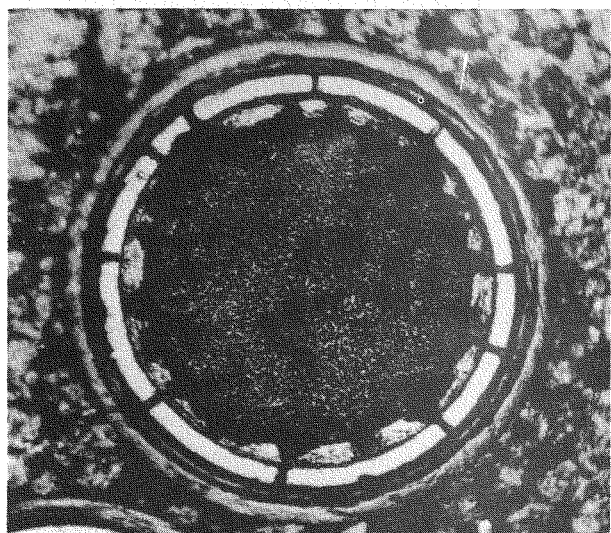


Fig. 31 HPD4/3B; Intact Kernel, Cracks in SiC Often Correspond with
Tips of Spearheads in Inner PyC Layer (X200)

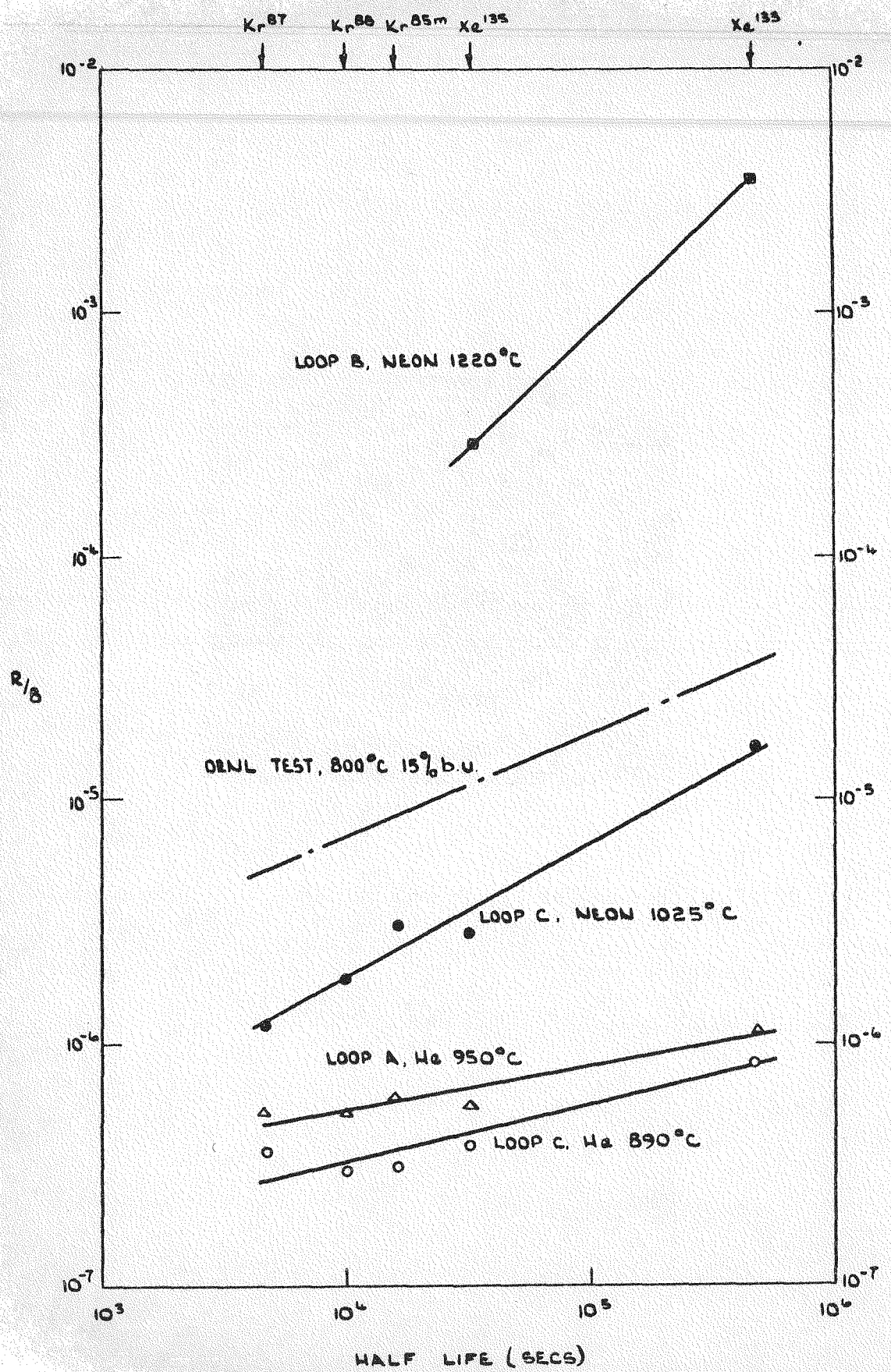


FIG. 32 PLOT OF RATIO OF RELEASE TO BIRTH RATE (R/B)
VERSUS HALF LIFE OF FISSION GASES IN STUDSVIK I